Analyses of a novel MGP-deficient mouse model to study MGP's N-terminal peptide via a transgenic approach

Lovely Yeasmin, BDS

Faculty of Dentistry

McGill University

Montreal, Quebec, Canada

January 2022

A thesis submitted to McGill University in partial fulfillment of the requirements of the degree of Master of Dental Sciences

Dedication

I dedicate this Thesis to my mother (Mrs. Hosneara Begum) and my sister (Dr. Eva Jesmin) for their unconditional support, love, and endless trust on me.

Acknowledgements

First, I would like to thank almighty God for giving me the knowledge and strength to dedicate myself and complete my research project in a satisfactory way. Without His blessing this journey would not have been possible.

I would like to express my most sincere and deepest gratitude to my supervisor Dr. Monzur Murshed, I admire his continuous support in my work and his dedication towards science and research. I learnt a great deal about research methodology, different experiments and data analysis in the past 2 years and hope to learn more in future from Dr. Murshed. I appreciate Dr. Murshed's compassion and dedication towards his students. I am thankful to my co-supervisor Dr. Philippe Campeau for his guidance and suggestions while pursuing my research. I am also thankful to my committee members Dr. Mari Kaartinen and Dr. Elaine C. Davis for giving me guidance and support for thesis completion during my committee meeting. My special thanks also go to Dr. Eva Jesmin and Sehrina Muzahid for always supporting me since the starting of my course at McGill University.

I am thankful to my current and past colleagues in my lab for their support, advice and help during my research time. Special thanks go to Haitham Al Quorain and Abhinav Parashar for their valuable advice and support. I am also thankful to Lina Abu Nada for giving me moral support and guiding me about thesis and I'm also grateful to Ophelie Gourgas for French translation of my abstract. I am grateful to my other colleagues, Kyoungmi Bak, Aish Scaria, Afroza Parvin, Ibrahim Sankour, Nwara Osman; for always being with me during my lab time and also supporting me in difficult times during different experiments. Special thanks go to my friend Dr. Nadia for reviewing my thesis.

I would also like to thank my “Faculty of Dentistry” friends Homa Fathi and Yatri, for making this journey even more enjoyable, and Crystal Noronha for her continuous help throughout the years in guiding me through the course.

My appreciation goes to the Shriners Hospitals for Children’s staff for making my days better, helping me in every step and for brightening my days with their smiles. Especial thanks goes to the animal facility technicians Mia Esser and Louise Marineau, for their impeccable work.

In the end I wish to acknowledge my family for supporting me in every step of my life and for encouraging me to work towards achieving my goal, especially my siblings who have always been with me, helping in my every decision making and during difficult times.

Table of Contents

List of Abbreviations

ABVG: Alcian blue-Van Gieson

ALPL: Alkaline phosphatase

AMP: Adenosine monophosphate

AS: Aortic stenosis

ATP: Adenosine triphosphate

BAV: Bicuspid aortic valve

BGP: Bone Gla protein

BMP-2: Bone morphogenic protein-2

BSP: Bone sialoprotein

Ca^{2+}: Calcium

CAC: Coronary artery calcium

CAVD: Calcific aortic valve disease

CKD: Chronic kidney disease

CVD: Cardiovascular disease

ECM: Extracellular matrix

ECCM: Extracellular matrix mineralization

ELN: Elastin

ENPPs: Ecto-nucleotide pyrophosphatase /phosphodiesterases

FGF23: Fibroblastgrowthfactor23

GACI: Generalized Arterial Calcification in Infancy

GAG: Glycosaminoglycans

GGCX: γ-glutamyl carboxylase

GLA: γ-carboxyglutamate

HA: Hydroxyapatite

KS: Keutel syndrome

MGP: Matrix Gla protein

Micro-CT: Micro-computed tomography

MVs: Matrix vesicles

OCP: Octa calcium phosphate

OPN: Osteopontin

P_i: Inorganic phosphate

PP_i: Pyrophosphate

PCR: Polymerase chain reaction

SOS: Spheno-occipital synchondrosis

TB: Toluidine blue

TNAP: Tissue non-specific alkaline phosphatase

VC: Vascular calcification

VKORC: Vitamin K epoxide reductase

VKVG: von kossa and van Gieson

VKDP: Vitamin K dependent protein

VSMCs: Vascular smooth muscle cells

XLH: X-linked hypophosphatemia

Abstract

Matrix Gla protein (MGP), an extracellular matrix (ECM) protein produced by both vascular smooth muscle cells and chondrocytes, is a potent mineralization inhibitor. The loss of function mutations in MGP cause Keutel syndrome, an autosomal recessive genetic disorder characterized by peripheral pulmonary stenosis, abnormal cartilage calcification and mid facial hypoplasia. MGP deficient mice faithfully recapitulate most of the anomalies seen in Keutel syndrome. While MGP's role as a mineralization inhibitor is well-established, until now its mode of action is not fully understood. Two sets of conserved residues in MGP – 4 glutamic acid and 3 serine residues, which undergo post translational modifications – are thought to be critical for MGP's anti-mineralization function. The conserved glutamic acid residues are post-translationally carboxylated to Gla residues. This occurs via an enzymatic process in a vitamin K-dependent manner. On the other hand, 3 conserved serine residues present at the N-terminal end of MGP are phosphorylated, although the kinase involved is currently unknown. Interestingly, bone Gla protein (BGP/osteocalcin), another skeletal Gla protein related to MGP, carries Gla residues, but does not show any anti-mineralization function in vivo. This observation suggests that there are additional structural feature(s) in MGP, which might be necessary to prevent ECM mineralization. Comparison of sequences of MGP and BGP mature proteins reveals that osteocalcin lacks the conserved serine residues of MGP. Based on this observation, as well as the published studies showing the anti-mineralization function of MGP's N-terminal peptides carrying the phosphorylated serine residues, I hypothesize that ***the addition of MGP's N terminal serine residues to BGP will confer the anti-mineralization function to BGP***. I will pursue a transgenic approach to test this hypothesis. To achieve this, I propose the following 2 aims:

Aim I: Characterize and analyze MGP-deficient *Mgp*$^{\Delta 55\text{-}62/\Delta 55\text{-}62}$mouse line.

Aim II: Generate transgene constructs to express modified BGP carrying MGP's serine residues.

Under Aim 1, I have characterized a novel mouse model *Mgp*$^{\Delta 55\text{-}62/\Delta 55\text{-}62}$ which carries a nonsense mutation preventing the translation of the mature protein. In this model, the tandem deletion of multiple nucleotides in the open reading frame of *Mgp* results in a stop codon (TGA) at the end of signal peptide. This model mimics the phenotypes of the original MGP-deficient mice (*Mgp-/-* mice) including the severe vascular calcification.

Under Aim 2, I have generated transgene constructs to express chimeric MGP-BGP proteins (*pSM22αMBgp*) in vivo. In these proteins, the N-terminal part of MGP carrying the serine residues will be fused with the unprocessed (pro protein) or the mature BGP protein. A *SM22* promoter has been added in this transgene which will drive the fusion protein expression in the vascular smooth muscle cells (VSMCs).

In future, the transgenic mice generated under Aim 2 can be mated with *Mgp*$^{\Delta 55\text{-}62/\Delta 55\text{-}62}$mice to generate *Mgp*$^{\Delta 55\text{-}62/\Delta 55\text{-}62}$*; SM22αMBgp* mice. These mice expressing the chimeric protein in the VSMCs can be analyzed to examine whether addition of the N-terminal sequence of MGP to BGP would be sufficient to prevent vascular calcification in the compound mutants.

Résumé

La protéine matricielle Gla (MGP), une protéine de la matrice extracellulaire (ECM) produite à la fois par les cellules musculaires lisses vasculaires et les chondrocytes, est un puissant inhibiteur de la minéralisation. Une mutation de perte de fonction dans MGP provoque le syndrome de Keutel, une maladie génétique autosomique récessive caractérisée par une calcification anormale du cartilage, une sténose pulmonaire périphérique et une hypoplasie faciale moyenne due à des mutations de perte de fonction dans MGP. Les souris déficientes en MGP récapitulent fidèlement la plupart des anomalies observées dans le syndrome de Keutel. Alors que le rôle de MGP en tant qu'inhibiteur de la minéralisation est bien établi, jusqu'à présent, son mode d'action n'est pas entièrement compris. Deux ensembles de résidus conservés dans MGP - 4 résidus d'acide glutamique et 3 résidus sérines, qui subissent des modifications post-traductionnelles - sont considérés comme essentiels pour la fonction anti-minéralisation de MGP. Les résidus d'acide glutamique conservés sont carboxylés post-traductionnellement en résidus Gla. Cela se produit via un processus enzymatique d'une manière dépendante de la vitamine K. D'autre part, les 3 résidus sérines conservés présents à l'extrémité N-terminale de MGP sont phosphorylés, par une kinase qui est actuellement inconnue. Fait intéressant, la protéine Gla osseuse (BGP/ostéocalcine), une autre protéine Gla squelettique liée à MGP, porte des résidus Gla, mais ne montre aucune fonction anti-minéralisation in vivo. Cette observation suggère qu'il existe des caractéristiques structurelles supplémentaires dans MGP qui pourraient être nécessaires pour empêcher la minéralisation de l'ECM.La comparaison des séquences des protéines matures MGP et BGP révèle que l'ostéocalcine est dépourvue des résidus sérines conservés de MGP. Sur la base de cette observation, ainsi que des études publiées montrant la fonction anti-minéralisation des peptides N-terminaux de MGP portant les résidus de sérine

phosphorylés, j'émets l'hypothèse que **l'ajout de résidus de sérine N-terminaux de MGP à BGP conférera la fonction anti-minéralisation à BGP**. Je vais poursuivre une approche transgénique pour tester cette hypothèse. Pour y parvenir, je propose les 2 objectifs suivants :

- Objectif I : Analyser et caractériser la lignée de souris *Mgp*$^{\Delta 55\text{-}62/\Delta 55\text{-}62}$ déficiente en MGP.
- Objectif II : Générer une lignée transgénique exprimant BGP modifiée.

Dans le cadre de l'objectif 1, j'ai caractérisé un nouveau modèle de souris *Mgp*$^{\Delta 55\text{-}62/\Delta 55\text{-}62}$qui porte une mutation non-sens empêchant la traduction de la protéine mature. Dans ce modèle, une mutation de substitution remplaçant une cytosine en adénine entraîne un codon stop (TGA) à l'extrémité du peptide signal. Ce modèle imite les phénotypes des souris originales déficientes en MGP (souris *Mgp-/-*), y compris une calcification vasculaire sévère.

Dans le cadre de l'objectif 2, j'ai généré des constructions transgéniques pour exprimer des protéines MGP-BGP chimériques (*pSM22αMBgp*). Dans ces protéines, la partie N-terminale de MGP portant les résidus sérine sera fusionnée avec la protéine BGP non transformée (pro protéine) ou mature. Un promoteur SM22 a été ajouté dans ce transgène qui pilotera l'expression de la protéine de fusion dans les cellules musculaires lisses vasculaires (VSMCs).

À l'avenir, les souris transgéniques générées sous l'objectif 2 pourront être accouplées avec des souris *Mgp*$^{\Delta 55\text{-}62/\Delta 55\text{-}62}$ pour générer des souris *Mgp*$^{\Delta 55\text{-}62/\Delta 55\text{-}62}$*;SM22-MBgp*. Ces souris exprimant la protéine chimérique dans les VSMCs peuvent être analysées pour examiner si l'addition de la séquence N-terminale de MGP à BGP serait suffisante pour empêcher la calcification vasculaire dans les mutants composés

Contribution of authors

Individual contributions to this thesis are as follows:

Lovely Yeasmin: All the analyses of the *Mgp*$^{\Delta 55\text{-}62/\Delta 55\text{-}62}$ mouse model; genotyped the model and setup breeding according to genotyping and finalized the *Mgp*$^{\Delta 55\text{-}62/\Delta 55\text{-}62}$ mouse line for breeding with transgenic mouse model. Second generated two transgene constructs; *pSM22αMBgp-1*and *pSM22αMBgp-2*; by preparing the DNA construct, purified it and send it for pronuclear injections.

Ophelie Gourgas: Initial screening of the *Mgp*$^{+/\Delta 55\text{-}62}$ founder mouse.

Dr. Philippe Campeau: Co-supervised the study.

Dr. Monzur Murshed: Conceptualized, designed, and supervised the study; aided in interpretation of the data.

Chapter1: General Introduction and Literature Review

1. Introduction and literature review:

Cardiovascular diseases (CVD) are one of the primary causes of death world-wide, specially the developed countries are the highest sufferers where, the death accounted by CVD is approximately 18 million per year [1]. CVD is the 2nd most important cause of death in Canada [2]. Arterial calcification found to be a major determinant of adverse cardiovascular events [3-5] as calcific deposits reduce the elasticity of the arterial walls impairing cardiovascular outcomes and may result in significant morbidity and mortality [6].

The calcific deposits in the arterial walls develop by deposition of calcium phosphate minerals in association with extracellular matrix (ECM). ECM is an essential compartment in the tissues of living organisms. While the ECMs in the 'hard' tissues of bones and teeth are normally mineralized, ECM mineralization is a pathological condition in the 'soft' tissues of the vertebrate organisms. Ectopic mineralization or calcification can occur in a variety of 'soft' tissues, which include but not limited to skin, blood vessel walls, kidneys and lungs [7]. These ectopic calcification events can cause a high prevalence of mortality and morbidity in patients with chronic diseases, such as chronic kidney diseases, diabetes, and atherosclerosis [8]. The following literature review will cover an overview of ECM mineralization and associated diseases with vascular calcification with a special focus on matrix Gla Protein (MGP).

1.1 ECM: Composition, organization, and function:

Cells are the building blocks of living organisms. They provide the basic structure of the body and are required for various specialized functions. Cells secrete different types of secretory materials into the micro-environment surrounding them. This extracellular micro-environment is composed of a three-dimensional network of macromolecules (collagens, enzymes, and glyco

proteins) and is collectively called as ECM (Figure A). ECM is an important component of cells, tissues and organs as it provides structural and functional supports to cells and tissues. Moreover, the ECM instructs significant morphological and physiological functions to elicit signal transduction and gene transcription regulations by binding growth factors and interacting with cell-surface receptors. Additionally, ECM undergoes continuous remodeling, and its molecular components encounter various post translational modifications [9]. The ECMs commonly constitute three major types of biomolecules, namely, glycosaminoglycans (GAGs), proteoglycans, and fibrous proteins. The ECM in a 'soft' tissue may contain fibrous proteins including collagen, elastin, fibronectin, vitronectin, and laminin. Among fibrillar proteins present in the ECM, collagen is the most abundant protein which accounts for 30% of total protein mass of living tissues [10] playing direct roles in tissue development, regulation of cell adhesion, and maintenance of tensile strength [11]. Collagen is first formed as procollagen which is secreted from different cells such as, fibroblasts, odontoblasts and osteoblasts in the extracellular spaces and converted into tropocollagen which later form fibrils. These fibrils give structural stability [12] and control the size and orientation of mineral crystals, and also promote cellular attachment, proliferation and differentiation. In addition, elastin and fibronectin are also important fibrous ECM proteins which facilitate recoiling of tissues and provide cellular traction forces. To induce the signals required for tissue morphogenesis, differentiation and homeostasis, as well as for physical scaffolding of the cellular constituents, an ECM is essential [9].

ECM of the 'hard' tissues, such as bone regulates cell proliferation, adhesion, differentiation, and responses to growth factors. Bone contains approximately 100 ECM proteins which have significant roles in its development and function [13]. Most of the weight of bone is made up of ECM which determines the skeleton properties in the vertebrates. Bone ECM is primarily formed

by collagen fibers and inorganic crystal salts of carbonated hydroxyapatites [$Ca_{10}(PO_4)_6(OH)_2$]. These crystal salts are formed by the reaction of calcium carbonate and calcium phosphate combining to create hydroxyapatite minerals, which undergo further reaction with magnesium hydroxide, fluoride, and sulfate to be crystallized. The mineralized collagen-rich ECM in bone is a composite material, which gives hardness, flexibility, and the load-bearing capacities to bones. To maintain healthy skeleton, remodeling of bone throughout life requires a balance between bone formation by osteoblast cells and bone resorption by osteoclast cells [14].

Another important organ carrying mineralized ECM in the craniofacial skeleton is tooth, an essential apparatus for mastication. Teeth are composed of 4 distinct tissues: three of them, e.g., enamel, dentine and cementum are mineralized, while the tooth pulp is a 'soft' tissue. Like bone, dentin and cementum are composed of collagen-rich mineralized scaffold. Although enamel carries hydroxyapatite minerals like bone, dentin and cementum, matured enamel carries very little organic matrix. Mineralization of teeth makes the structure hard (enamel is the hardest tissue of the body that covers the crown part of tooth of mammals) and able to withstand force of mastication, preventing mechanical abrasion and chemical attack [15].

ECM in blood vessels is formed primarily by vascular smooth muscle cells (VSMCs), fibroblasts and endothelial cells. Major vessel wall proteins are elastin, collagen, fibronectin, fibrillin, fibulin and thrombospondin. In the major aortas, elastin and microfibrillar proteins are arranged in concentric layers of protein scaffolds known as elastic laminae. Layers of collagens are deposited to the regions adjacent to the elastic laminae. The VSMCs and fibroblasts are present in between the elastic lamina/collagen scaffolds. The middle part of the blood vessel carrying the concentric layers of elastic lamina/collagen scaffolds and cells are known as the medial layer. The endothelial cells present in the intimal layer of the vessels contribute to the formation of the

innermost elastic lamina adjacent to the lumen. The outer most part of the blood vessels is known as adventitia (Figure B). Both the medial and the intimal layers of blood vessels can be affected by pathologic mineral deposition.

1.2 ECM mineralization (ECMM):

ECMM is a physiological process for hard tissues like bone, teeth, and hypertrophic cartilages. It is important for providing mechanical stability to the skeletal and dental tissues and needed for maintenance of body structure, protection of soft organs inside the body, providing locomotion, helping in mastication. In addition, mineralized bone serves as a reservoir for the calcium and phosphate ions. In bone, the mineralization of the extracellular collagen scaffold is regulated directly by osteoblasts (bone forming cells), and to some extent by osteocytes via the regulation of inorganic phosphate homeostasis in the body [15].

ECMM in the 'soft' tissues is essentially a pathological process. Such calcification events may affect the blood vessels, heart valves, skin, subcutis, and joints. Vascular calcification can increase the risk of mortality and morbidity for human beings. On the other hand, joint calcification can impair the mobility and can lead to destruction of the compromised tissues [16]. It is important to understand the determinants of ECMM to develop therapeutic approaches for various pathologies associated with ECMM.

1.2.1 Proteins regulating ECMM:

ECMM has a prime role in bone and cartilage formation. Some skeletal ECM proteins carry γ-carboxylated glutamic acid (Gla) residues which are essential for their functioning. These proteins are mainly present in the bony matrix, dentine and other tissues that are calcified. Osteocalcin (BGP), matrix Gla protein (MGP) and periostin are mainly the Gla containing

proteins. These proteins have different important functions, for example, serum osteocalcin concentration can be used as a biochemical parameter for bone formation, MGP can act as a bone mineralization inhibitor and periostin can maintain the bone strength by participating in collagen folding and fibrinogenesis [17]. Osteonectin is present in mineralized tissues and abundantly expressed by osteoblasts. It regulates the release of calcium ions by binding with collagen and hydroxyapatite crystals which control collagen mineralization during bone formation [18]. Bone sialoprotein (BSP) is a vastly glycosylated non-collagenous phosphoprotein which binds to both hydroxyapatite and collagen type I. BSP has been proposed to regulate the differentiation of osteoblast and commencement of matrix mineralization in bone tissue [19]. Likewise, another related protein OPN has also been suggested to regulate the mineralization of bone. In bone remodeling, OPN contributes to bone resorption by regulating osteoclastogenesis and osteoclast activity [20].

Mechanical and biochemical properties of ECMM are involved in regulating cell adhesion, proliferation, differentiation, thus exhibits the functional characteristics of the mature bone. Formation of new bone during regeneration is regulated by chondrocytes, osteoblast, osteocytes, and osteoclasts [17].

1.3 ECMM of soft tissues:

Ectopic mineral deposition on the extracellular scaffold leads to ECMM in the soft tissues, which is often regarded as a risk factor for many life-threatening diseases. It is a pathological biomineralization occurring in soft tissues and is typically composed of calcium phosphate salts, including hydroxyapatite, but can also consist of calcium oxalates and octacalcium phosphate. Systemic mineral imbalance in ectopic calcification is leading to dystrophic calcification which may cause tissue alteration and necrosis. Although all soft tissues undergo mineralization, but

most commonly affected tissues are skin, tendons, and some cartilaginous and cardiovascular tissues [22].

1.3.1 Vascular cells and ECM:

Among different types of soft tissue calcification events, cardiovascular tissue mineralization leads to the most significant amount of morbidity and mortality. In vascular calcification, deposition of calcium minerals occurs in the major arteries which reduces the elasticity of the aorta and arteries and impairs cardiovascular hemodynamics as well as aortic stenosis, cardiac hypertrophy, myocardial ischemia and lower-limb vascular insufficiency, congestive heart failure and compromised fundamental activities of the cardiovascular system [16]. These consequences arise due to progressive age, uncontrolled blood sugar, hypercholesterolemia, pathological valve conditions, chronic renal insufficiency and infectious as well as inflammatory injuries.

Smooth muscle (SM) cell is a special type of cell involved in vascular calcification. Its contractile, involuntary functions play a vital role for the functioning of blood vessels and maintain blood pressure and also maintains and allows remodelling of ECM of blood vessels. These cells are found in different tissue types, such as, blood vessels, trachea, the digestive tract, urinary bladder, and iris. Recent evidences suggest that, SM cells are able to display features of osteoblasts, chondrocytes, adipocytes, and macrophage foam cells [17]. SM has highly specialized function which are contraction and relaxation. It regulates the movement of body fluids through hollow and tubular organs. SM cells consist of large amounts of ECM which can constitute >50% of the media volume of large elastic arteries [18]. SM cells do not have striations and sarcomeres, but they produce connective tissue called endomysium, they also contain contractile proteins, such as, actin and myosin, and thick and thin filaments. SM cells

mitotically divide to produce new cells and can undergo hyperplasia. Contraction of SM is triggered by Ca^{++} ions binding to intracellular calmodulin which then activates an enzyme called myosin kinase that phosphorylates myosin heads so they can form the cross-bridges with actin and then pull on the thin filaments. It is found throughout arteries and veins where it plays a significant role for regulation of blood flow, blood pressure and tissue oxygenation.

VSMCs are the important constituent of blood vessels and mostly found in the medial part of the blood vessel (tunica media) where they are organized around the vascular lumen forming numerous layers. The tunica media is positioned between tunica intima and tunica adventitia which is separated by lamina elastic internal and lamina elastic external [19]. In different vascular beds VSMCs show complex pattern of development. VSMCs arise from diverse embryonic tissues including the mesothelium, the neural crest, the pro epicardium, and the somites, give rise to VSMCs [18]. Smooth muscle of healthy blood vessels has considerable plasticity which is largely contractile that helps in blood pressure autoregulation. However, during the life span vascular cells change into non-contractile and synthetic cells and develop to atherosclerosis or vessel remodeling due to proinflammatory stimuli, diet or other factors [20]. Functions of VSMCs include vascular repair functions, hemodynamics regulation, structural support, and are major contributors to SM and vessel renewal through differentiation in the event of an injury. VSMCs are a highly specialized cell with a high degree of plasticity. In adult blood vessels these cells proliferate at an extremely low rate and also exhibit very low synthetic activity and express a unique sets of contractile proteins, ion channels and signaling molecules essential for the cell that is distinctive in comparison to other cell types. [21]. In the vessel wall VSMC is the most abundant cell type and most important functions are contractility and regularity of blood vessel tone, blood flow and blood pressure in the vessel wall. In

cardiovascular pathologies it plays a central role such as, atherogenesis, hypertensive vasculopathy, and transplantation arteriopathy [22]. VSMCs carry out biosynthetic, proliferative, and contractile roles, characterized by production of ECM components, an increased rate of proliferation, relocation, and reduction of VSMCs-specific markers. In most systemic arteries VSMCs contribute to vasodilation to maintain oxygen supply to the tissues [23].

Endothelial cells in the intimal layer are situated upon a basement membrane where laminin, entactin, fibronectin and type IV collagen are more abundant. In the media, basement membrane surround each smooth muscle cells (SMCs) where fibronectin, fibrillar types I, III, and V collagen, type XVIII collagen, and proteoglycans are embedded [24].

1.3.2 Calcification of vascular ECM

It has been suggested that matrix vesicles (MVs) serve as nucleation sites for hydroxyapatite in the skeletal and vascular tissues. The MVs are membrane-bound bodies originated from the plasma membrane of the cells involved in ECM mineralization. These vesicular bodies provide enclosed micro-environments may occur. The vascular cells may undergo chondrogenic/osteogenic differentiation and initiate the mineralization of the surrounding ECMs via the MVs (Figure C). It has been suggested that normally, calcification does not take place in the VSMC-derived vesicles because of the presence of some mineralization inhibitors, such as, MGP and Fetuin-A [25].

Adoptions of chondrogenic/osteogenic features by the cells in vascular walls are known to be an important mechanism by which vascular tissues undergo mineralization. FGF-2 and BMP play important role in vascular calcification by stimulation of Cbfa1/Runx2 activity which is a distinct transcription factor for chondrocytic/osteoblastic differentiation [26]. Mineralization of VSMCs accelerates due to elevated extracellular calcium phosphate deposition which is linked to the

induction of Cbfa1/Runx2; and increase in bone-linked proteins such as OC, OPN, and alkaline phosphatase (ALP) [27, 28].

According to deposition sites of minerals, vascular calcification can be categorized as 4 histo-anatomic variants: calcification of medial artery, calcification of atherosclerotic intimal layer, cardiac valve calcification, and soft tissue calciphylaxis [3]. Medial artery calcification is a highly specific vascular injury which alters vascular compliance and may lead to amputation and cardiovascular mortality [29].

1.4 Major diseases associated with vascular calcification:

Soft tissue calcification can result from injury or inflammatory reaction precipitated by trauma, repetitive frictional motion, infection, autoimmune illness. Soft tissue calcification is a pathological mineralization which has been the derivative of several clinical conditions which leads to significant morbidity and mortality [30]. Below discussed some genetic and chronic diseases, which are mostly related to soft tissue calcification (Figure D):

1.4.1 Atherosclerosis:

Atherosclerosis is one of the most important causes of vascular disease which is the major contributor of ischemic heart disease or ischemic stroke along with peripheral arterial disease [31]. Vascular calcification is closely linked to atherosclerosis and can occur in either the intimal or medial layers of the arterial wall. Atherosclerosis-related intimal calcification is processed by lipid accumulation, inflammatory reactions, intimal thickening due to fibrosis, focal plaques development and endothelial dysfunction [25, 32-34] (Figure C). Atherosclerotic lesions can begin at an early age and accelerate as the disease advances and progressively becomes calcified [35]. Several factors are responsible for the development of atherosclerosis, including ageing,

diabetes and family history are the leading risk factors [25]. Bostrom et al, highlighted the expression of BMP2 in calcifying atherosclerotic plaques for the first time, where it had been observed that active osteogenic process contributes to vascular calcification [29, 36-38]. BMP2 regulates all histo-anatomic variants of vascular calcification. This calcification is of dystrophic type which is characterized by cellular necrosis, inflammation, alterations of lipoproteins and phospholipids, release of apoptotic bodies and debris of dead macrophages and VSMCs causing micro calcification in the atherosclerotic plaque [29, 35, 39]. The apoptotic bodies and matrix vesicles, derived from VSMCs and macrophages, provides with the initial calcium-phosphate crystals deposits, which eventually form hydroxyapatite crystals. [40]. Calcification of atherosclerotic neo-intima is due to micro calcifications which is defined as small calcium deposits and formed by debris of necrotic or apoptotic cell death within the lipid core. Subsequent formation of macro calcification results in plaque stabilization [35].

1.4.2 Chronic kidney disease (CKD):

CKD patients are in a much higher risk of developing vascular disease [41]. In CKD, calcification is accelerated in association with atherosclerotic lesions in the intima of the arterial vessel wall and the medial layer which is called Mönckeberg's sclerosis [42]. The major constituent of the medial arterial layer is the medial layer which undergoes vascular calcification due to disturbance in Ca^{2+} and P^{2-} metabolism. Cardiovascular mortality in CKD patients results from hyperphosphatemia and elevated minerals of calcium and phosphorus compounds. Amorphous mineral formation in Monckeberg's sclerosis occurs along with or within one or more elastic lamellae of the medial layer [43] (Figure C), this is also named as medial artery calcification which is more common in patients with diabetes and CKD [44]. In patients with CKD dysregulation in Ca^{2+} and serum phosphate (P^{2-}) metabolism has an important role in the

progression of vascular mineralization. CKD patients have a disproportionately high occurrence of vascular calcification compared with the healthy population [27]. In addition, these patients also exhibit higher risk of cardiovascular mortality and accelerated medial calcification in dialysis cases. In CKD, phosphate and calcium imbalance may promote VSMC dysfunction. Elevated levels of phosphate and calcium promote calcification of VSMC. Loss of inhibitor function development of a calcifiable ECM is accompanied by osteo/chondrogenic differentiation of VSMC [45]. Vascular calcification in patients with advanced kidney dysfunction, develop hyperphosphatemia secondary to impaired renal excretion of phosphate, and leads to transformation of VSMC into osteoblast type cells which take part in the tissue mineralization process [46].

1.4.3 Calcific aortic valve disease (CAVD):

CAVD is the most prevalent valve disease and a major health problem with high morbidity and mortality. Risk factors of CAVD are diabetes mellitus, hypertension, smoking, elevated cholesterol, and genetic and developmental origins. Bicuspid aortic valve (BAV) disease may lead to CAVD via the irregularities of RUNX2 expression [47-49]. Pathophysiology of CAVD can cause aortic stenosis (AS), the most common heart valve disease which occurs due to focal ectopic calcification and extensive fibrous thickening of the valve leaflets. The clinical feature of AS is degenerative calcification, congenital bicuspid valve, rheumatic changes. This valve calcification is irreversible [50]. Production or degradation steadiness of ECM components is responsible for CAVD pathogenesis. Aortic valve cells acquire an osteoblast-like phenotype and account for calcium crystal organization in lamellar bone type structures. It undergoes micro calcification process and form about 85% amorphous diffuse type of calcified mass in the valve. Two mechanisms may trigger CAVD one of them is mechanical stress of endothelium, and the

other is lipid deposition. Lipid oxidation can occur via either enzymatic or non-enzymatic processes. Remodeling of abnormal ECM is crucial for CAVD. There are two types of calcifications seen in CAVD, which are the dystrophic calcification, and the other is bio-mineralization/ossification. The first step occurs as an osteoblast free mechanism, also known as diffuse calcification of myofibroblast differentiation. Dystrophic calcifications happen due to abnormal collagen and passive deposition of hydroxyapatite [51, 52]. It has been observed that mice which are lacking in major ECM proteins exhibit developmental defects in valve formation and function [52]. Mice deficient of elastin do not survive after birth due to vascular obstruction, whereas heterozygous elastin mice undergo aortic valve abnormalities in adulthood [53-55]. More studies show that mutations in a several types of ECM genes are associated with progressive valve dysfunction and aortic valve malformations. Marfan syndrome is caused by mutations in the FIBRILLIN-1 gene [56, 57]. In this syndrome infants have severe mitral and tricuspid regurgitation, leads to aortic root dilatation. Due to progressive valve dysfunction, long term prognosis of Marfan syndrome is poor [58]. Mutations in COL1A1 patients are associated with osteogenesis imperfect which may cause prolapse of aortic and mitral valve [49, 59].

1.4.4 Generalized arterial calcification in infancy:

Generalized arterial calcification in infancy (GACI) is an uncommon but life-threatening genetic disorder also known as idiopathic infantile arterial calcification which is primarily caused by mutations in the *ENPP1* gene [60]. It is a genetic ectopic mineralization disorder, which causes diffuse arterial calcifications [61]. Pyrophosphate inhibits nucleation and epitaxial calcification, which generate via a family of three ectonucleotide pyrophosphatase/phosphodiesterase (ENPPs). *ENPP1* is a type II extracellular transmembrane glycoprotein expressed in different cell types including osteoblasts, osteoclasts, chondrocytes and VSMCs. It regulates vascular

calcification**,** vascular tone, inflammation, and remodeling. *ENPP1* has a role in inhibiting calcification in soft tissues and a lack of *ENPP1* can cause development of spontaneous aortic calcification in infants. It contributes to degenerative dystrophic valvular calcification [29]. Its primary function is to hydrolyzes extracellular adenosine triphosphate (ATP) to produce adenosine monophosphate (AMP) and inorganic pyrophosphate (PPi). PPi is a significant inhibitor of hydroxyapatite formation and vascular calcification, deficiency of *ENPP1* results in reduced formation of extracellular PPi which causes ectopic calcification. In case of GACI patients, this calcification occurs specifically in the vascular internal elastic lamina due to severe myo-intimal growth and reduced vascular elasticity causes arterial stenosis which leads to hypertension, myocardial ischemia, and heart failure. Arteries often show calcium deposition and fibro intimal hyperplasia which can contribute to narrowing luminal structure. GACI is associated with a high mortality rate from vascular occlusion and additional cardiovascular complications [62-64].

1.4.5 Keutel Syndrome (KS):

KS is an exceptional autosomal recessive disorder, which was first reported by Keutel J. in 1971. This condition is predominantly found in children of consanguineous parents. It is usually diagnosed during childhood and characterized by atypical cartilage calcification, peripheral pulmonary stenosis, midfacial hypoplasia with flattening of the nasal bridge, short distal phalanges and cardiovascular calcification defects [65]. These clinical traits are highly variable in their severity and occurrence. KS is caused by the loss of functioning of mutation in the matrix Gla protein. Matrix Gla protein is an extracellular protein which is a potent ECM mineralization inhibitor for vascular and cartilage calcification and is expressed by chondrocyte and vascular smooth muscle cells [66]. KS is a rare genetic disease with only 37 cases confirmed in

worldwide [67], KS patients life expectancy depends on respiratory complications which usually treated with bronchodilators and corticosteroids [68, 69]. Dr. Karsenty's group generated matrix Gla protein knockout ($Mgp^{-/-}$) mice which were used as a model for KS [70]. These mice faithfully recapitulate some traits of KS patients such as various cartilaginous tissues and severe vascular calcification [69-72]. Consequently, $Mgp^{-/-}$ mice die before they reach two months of age due to massive aortic calcifications and subsequent vessel wall rupture [70].

1.5 Inhibitors of ECMM:

Soft tissue mineralization (commonly known as ectopic mineralization) depends on multiple factors. The most common cause involves the role of mineralization inhibitors. These inhibitors are of two types: First there are small inorganic molecules, such as inorganic pyrophosphate and another type is composed of proteins, such as matrix Gla protein (MGP), osteopontin and fetuin-A (Figure B).

These mineralization inhibitors are either less abundant or are enzymatically inactivated in bones or hard tissues so that the process of ECM mineralization can initiate and progress [7]. Serum inorganic phosphate (Pi) plays an important role in hard tissues like bone and teeth. Low Pi level (hypophosphatemia) is associated with some diseases such as rickets or X-linked hypophosphatemia (XLH). Hypophosphatemia can also lead to ectopic calcification in medial calcification [73, 74]. In vitro studies showed that high phosphate levels can cause further mineralization of ECM secreted by VSMC and osteogenic differentiation of these cells. Moreover, presence of bone markers such as osteopontin (opn), tissue non-specific alkaline phosphatase (TNAP) and bone morphogenic protein-2(BMP-2) confirmed that these cells acquire osteoblastic like characteristic [8, 75, 76]. In the elastic lamina of the arterial wall showed abnormal calcification due to some ECM protein (Figure C) [77-80]. Some proteins which

prevent ECM mineralization include Matrix Gla Protein (Discussed in bellow) FetuinA (alpha 2 - Heremans-Schmid glycoprotein). Fetuin-A mainly inhibits formation of calcium phosphate crystal instead of dissolving crystalline structures [77].

1.6 MGP and its structure:

MGP is a small (~14-kDa protein) secretory and vitamin K-dependent (VKDP) protein which was first isolated from demineralized bovine bone matrix and characterized by Price et al. in 1985 [81]. It was found to be significantly involved in the inhibition of ECMM, particularly in the cartilaginous tissues. Although this protein is found in multiple tissues such as, bone, heart, kidney and lungs, higher expression was found in the vascular walls and cartilaginous tissues [70]. Primary structure of MGP contains a 19 amino acid signal peptide some of which is partly conserved in the orthologs. In addition, N-terminal part of mature MGP has a domain of phosphorylation (SxxSxxS) which is followed by a conserved cleavage site identified by the consensus sequence AxxF(Figure E). A conserved γ-carboxylase recognition site is also included in this N-terminal site. MGP contains another cleavage site close to its carboxy-terminal end in between two conserved arginine residues (RR) or an arginine and a glycine (RG) [82-84]. Four (out of five in human) of the γ-carboxyglutamate residues and the two conserved cysteines are located between AxxF and RR/RG cleavage sites [84, 85]. The human gene spans 3.9 kbs of chromosomal DNA is located on chromosome 12p13).1–12.3 which codes for the 103 amino acid full-length protein. The cleavage of the 19 amino acid signal peptide results in the mature protein spanning from residues 20–96. There are two sets of conserved residues – 5 glutamic acid residues (4 in mice) and 3 serine residues which undergo post-translational modifications (Figure F).

1.6.1 Deficiency of MGP and vascular calcification:

Deficiency of MGP cause keutel syndrome in humans, a rare autosomal disease (described in section 1.7.5) characterized by diffuse ectopic calcification. Considering their abundance in the skeletal tissues, MGP (in cartilage) and a related protein osteocalcin (in bone) have been identified as the skeletal Gla proteins. *Mgp* null (*Mgp-/-)* mice shows most of the phenotypic features of this disorder [70]. Later, Murshed*et. al.* showed that *Mgp* expression in VSMC corrects arterial calcification[71] .Transgenic over expression of MGP *in Mgp-/-;SM-22-Mgp* mice model fully transverses the vascular calcification phenotype [86].

1.6.2 Absence of chondrogenic/osteogenic differentiation of VSMCs in MGP-deficient arteries:

Previous studies reported that MGP inhibits BMP2 signaling which acts as an up regulator of chondrogenic/osteogenic differentiation of VSMCs [87]. However, using both molecular biology and transgenic approaches Khavandgar et al convincingly demonstrated that chondrogenic or osteogenic differentiation of VSMCs is not a prerequisite for ECMM in the arteries of MGP deficient mice. This study did not find any up regulation of skeletal tissue-specific markers in the MGP-deficient arteries. Moreover, ablation of alkaline phosphatase, a key enzyme required for bone, cartilage, and tooth mineralization, and a downstream effector of BMP2 signaling, did not prevent the initiation and progression of vascular calcification in MGP-deficient mice. These results convincingly demonstrated that BMP2 signaling is not involved in the observed vascular calcification in this model. Also, when a lacZ reporter transgene expressed in chondrocytes was introduced to the *Mgp-/-* mice, there was no expression of the reporter in the VSMCs. Collectively, these results suggest that the observed vascular calcification trait seen in *Mgp-/-*

mouse is independent of any chodrogenic or osteogenic differentiation of VSMCs. Instead this paper demonstrated that the vascular calcification in these mice is dependent on the amount of elastin, a major elastic lamina protein present in the arterial tissues [88]. The overall suggestion of this paper is that the local action of MGP prevents medial elastic lamina calcification (elastocalcinosis).

1.6.3 Deficiency of MGP and craniofacial anomalies:

Multiple genetic mutations are linked with craniofacial malformations. In this regard, fibroblast growth factor signaling affected by autosomal dominant mutations observed midface hypoplasia in several diseases, namely, Crouzon syndrome, Pfeiffer syndrome, Apert syndrome and others[89, 90]. In these diseases, premature fusion of the cranial sutures remained the principal cause of midface abnormalities, where there is premature closure of the cranial base synchondroses [91, 92]. Studies found that midface hypoplasia in MGP-deficient mice is primarily precipitated by impaired growth of the maxillary and palatine bones and also associated with irregular mineralization and limited of the nasal septum growth; in these cases, it had been demonstrated that, lack of MGP is responsible for the septal chondrocytes which undergoes apoptosis. In this region, the mechanism of cartilage mineralization is different to endochondral bones, where differentiation of hypertrophic chondrocytes is not required. Study results have showed that the extent of ectopic nasal septum mineralization in the MGP deficient background is dependent phosphate concentration, where body phosphate level reduction hinders nasal septum mineralization thus prevents craniofacial malformations.

1.7 post-translational modifications of MGP:

MGP undergoes at least four post translational modifications to generate a mature protein. The

four post-translational modifications are: cleavage of the signal peptide, carboxylation of glutamic acid residues, Phosphorylation of serine residues and formation of Disulphide Bridge, as shown in (Figure F). γ-Carboxylation of Glu occurs at residues 21,56,60,67, and 71 of the full-length protein. Serine residues at positions 22, 25, and 28 of the full-length protein, located in the N-terminus of the mature protein [81, 93]. MGP in human contains five glutamic acid (Gla) residues at positions 37, 41, 48 24 and 52 and in mice contains 4 Gla residues and it belongs to a family of vitamin K-dependent proteins which undergo post-translational gamma-carboxylation to become activated to fulfill its calcification inhibitory function. This carboxylation step cannot take place in the absence of vitamin K, which has an unequivocal role in driving this post-translational step [41, 94]. In addition, its glutamic acid residues play a role to bind Ca^{++} ions and hydroxyapatite minerals which give MGP its mineral binding capacity (Figure E). In different domains, mature MGP have different functions but among them most important function is inhibition of ECM mineralization.

1.7.1 Cleavage of the signal peptide:

MGP protein sequence has a signal peptide sequence which contains 19 amino acid residues which is required for its translocation in endoplasmic reticulum. This signal peptide is cleaved at the position of cysteine and the mature protein is exported into the cell [95] (Figure F).

1.7.2 post-translational modification of glutamic acid residues:

MGP's glutamic acid residues undergoes gamma carboxylation by the help of two enzymes, the one is gamma glutamyl carboxylase (GGCX) and the other one is vitamin K epoxide reductase (VKORC) [96]. The reduced form of vitamin K acts as an indispensable co-factor for carboxylation of glutamic acid residues (Glu) to gamma glutamic acid or Gla residues. After

reduction, vitamin K can be recycled by the vitamin K epoxide reductase (VKOR), which oxidizes it to reinitiate the cycle. This vitamin K co-factor is inhibited by vitamin K antagonists such as Warfarin, (Figure G) which is commonly prescribed to patients as an anti-coagulant. Treatment with warfarin leads to decrease in skeletal Gla proteins production, growth impedance of newborn rats and hypertrophic zone of growth plate cartilage where *Mgp* has been shown to be expressed [97]. Price *et al.* showed that through inhibition of the γ-glutamyl carboxylation of MGP of 3–5 weeks old rats by warfarin induced calcification of the elastic lamellae in arteries and heart valves [96, 98-101].

Another bone protein which also contain Gla residues called bone Gla protein (BGP) undergoes gamma-carboxylation and both protein (BGP and MGP) contain a Glu-X-X-X-Glu-X-Cys structure and are vitamin K dependent proteins [102]. Understanding the difference of 2 Gla containing protein for controlling of ECM mineralization different knockout model has been constructed. In 1997, Karsenty's lab generated *Mgp-/-* mice for understanding the role of MGP in ECM mineralization and the molecular determinants which regulate this process and also Murshed et al, constructed different transgene and knockout models to understand the role of these two Gla containing proteins [70, 71, 103]. Despite, MGP and BGP proteins share common structural motifs, for example, the Gla residues, they appear to play different roles in tissue mineralization. MGP shows anti-mineralization function whereas BGP does not. BGP is a small secretory protein synthesized as a pre-propeptide. It is separated from organic matrix of bovine bone and secreted by osteoblasts and odontoblasts [104]. It contains Gla residues (Figure I) but does not have any serine residues as like MGP sequence. It is involved in hormonal function, regulation of metabolism, and fertility [105-108]. Though BGP is a bone protein and contain Gla residues but yet its deletion in mouse did not show abnormal ECM mineralization in MGP

knockout mice71 [71, 109]. In addition, MGP's local expression can completely rescue the vascular calcification phenotype in *Mgp-/-* mice, whereas BGP expression in the VSMCs of these mice does not prevent arterial calcification [71].

1.7.3 Serine phosphorylation of MGP:

MGP's another post-translational modification is serine phosphorylation, which is thought to play a significant role for regulation of protein secretion to the extracellular space. This phosphorylation happens at the position of 3, 6 and 9 of MGP sequence [96] by an yet unknown kinase [110, 111] (Figure H). MGP peptides carrying the phosphorylated serine residues were shown to bind to calcium crystals and inhibit the nucleation process of hydroxyapatite salts. In vitro studies demonstrated that MGP's N-terminal peptide carrying phosphorylated serine residues can prevent mineral deposition, while the same peptide when carried unphosphorylated serine residues did not show any anti-mineralization properties [112].

1.7.4 Disulphide bridge formation:

Another post-translational modification takes place in MGP protein sequence at the position of 54 and 60, where internal disulphide bond form in between two cysteine amino acids [113] (Figure F).

1.8 CRISPR/Cas9 genome editing technology:

The recent advances in genetic engineering and the use of animal models have tremendously enhanced our ability to study various disease processes and paved the path towards treatment of many pathological conditions. Among various genetic engineering technologies, the transgenic approach refers to the process of alteration of genome by introducing biologically non-existing

DNA into a genome of a host organism [114]. The recent discovery of a bacterial pathway to specifically target bacteriophages by means of its clustered regularly interspaced short palindromic repeats (CRISPR) in the genome and the nucleases (e.g. Cas9) associated with the CRISPR coded RNAs has provided novel tools for targeted DNA modifications. This method requires a short synthetic guide RNA (gRNA) which carries a sequence complementary to a target sequence (to be modified) and also a sequence to recruit the Cas9 nuclease. The gRNA and the Cas9 protein are introduced to the nucleus of a fertilized egg to create a double stranded break in the genomic DNA. The specificity of the break site is determined by the complementary sequence present in the gRNA, which is immediately followed by a protospacer motif, also known as a PAM sequence (NGG). In the presence of an exogenously given single stranded template (ssODN) with flanking sequences encompassing the break site and also carrying the desired mutations, the target sequence can be modified as desired. In the absence of the ssODN, the double stranded break can be repaired by a method known as non-homologous end joining which may introduce some random insertions or deletions (collectively knowns as 'indels') at the break site. Even when the gRNA, Cas9 nuclease and the ssODN are co-injected into the nucleus of a fertilized egg, in some rare cases, there might be non-homologous end joining without involving the ssDNA-mediated repair process. This later event has implication on the current work [115, 116].

1.9 Figures:

Figure A

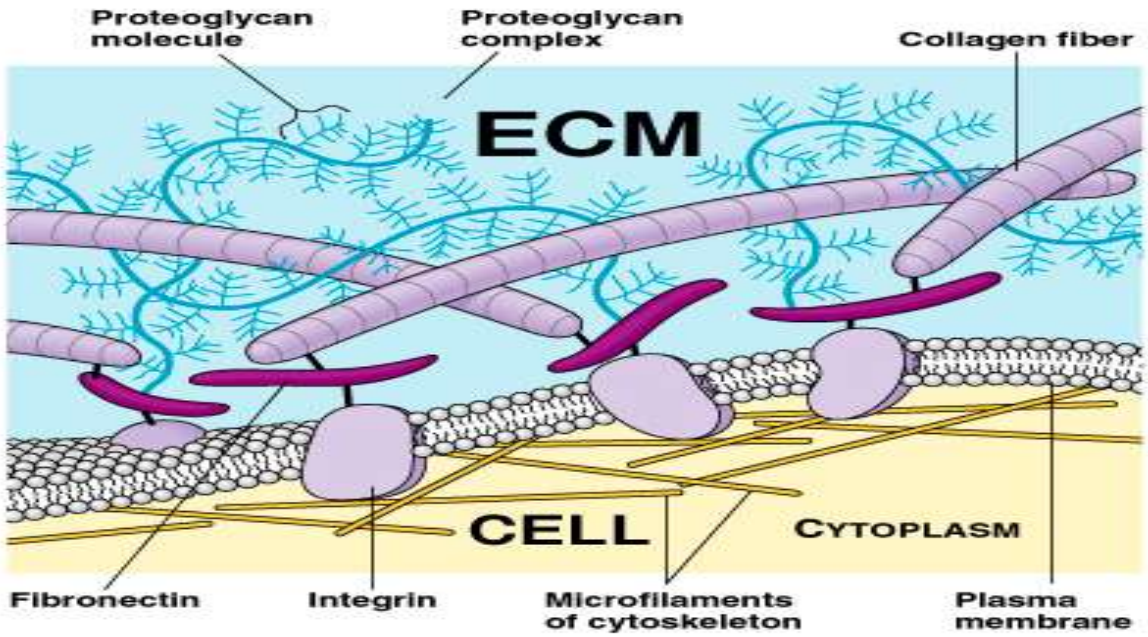

Figure A: ECM formed by three-dimensional network.
Ref: Dr. Jacques Imbeau; Integrative IDM

Figure B:

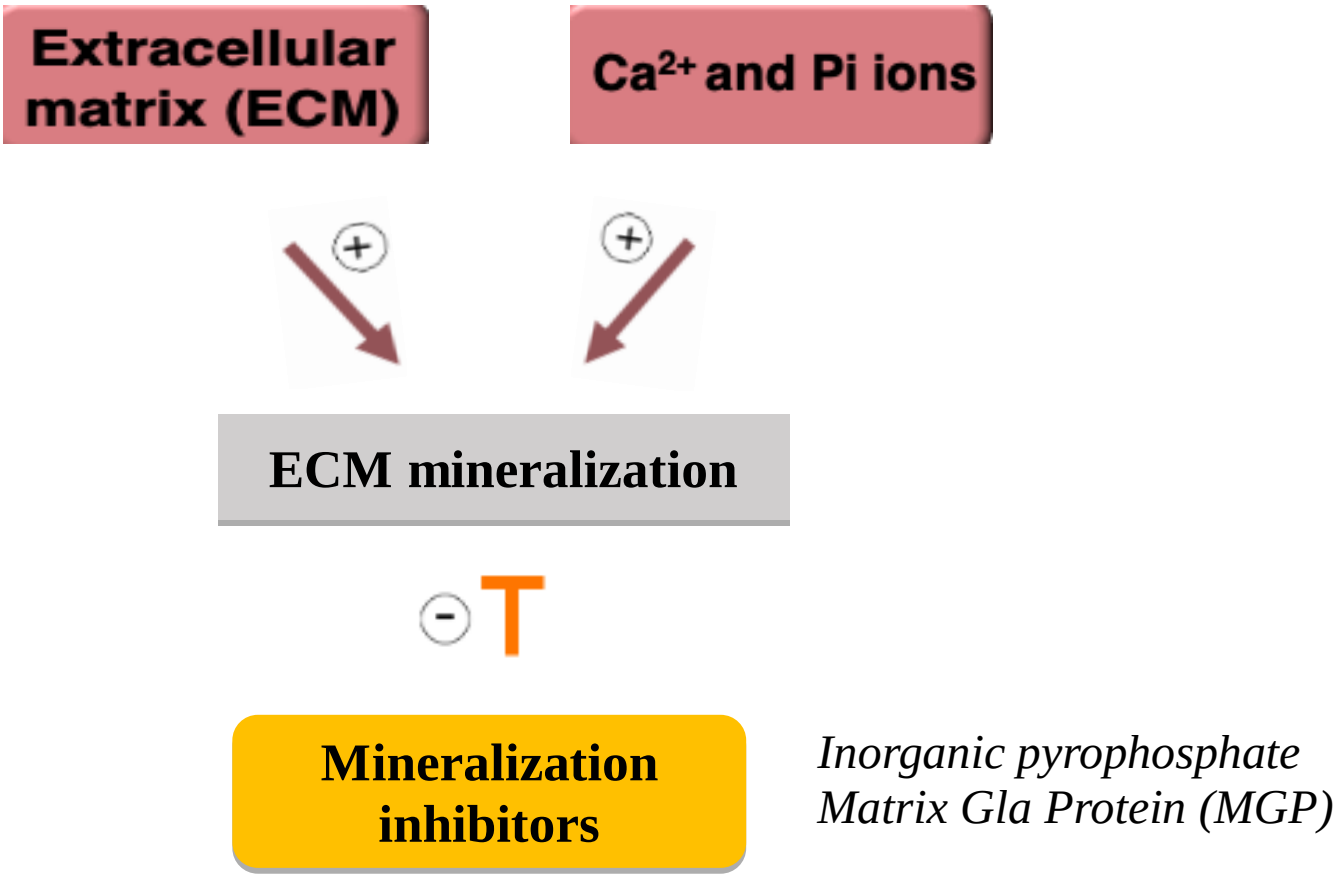

Figure B: Schematic representation of ECM and mineralization. Determinants of ECM mineralization inhibitor. Calcium and phosphate accumulation cause ECM mineralization. Inorganic pyrophosphate, Matrix Gla Protein inhibits such mineralization.

Figure C

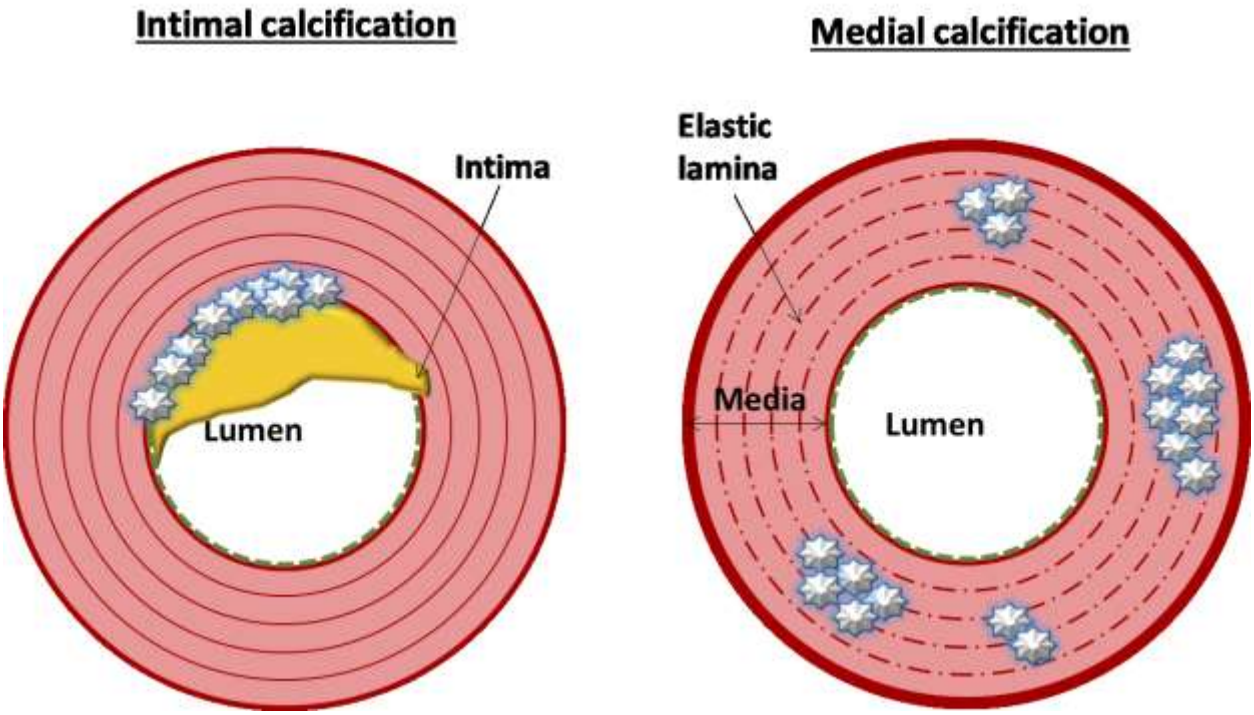

Figure C: Intima vs media aortic calcification. Schematic representation of intima and medial calcification. Minerals deposit on the intima layer in association with the atherosclerotic plaque in intima calcification. In media calcification, mineral crystals are deposited on the elastic lamina. Also, thickening of the media and fragmentation of the elastic lamina is observed (Adapted from Dr. Murshed's lecture slides)

Figure D

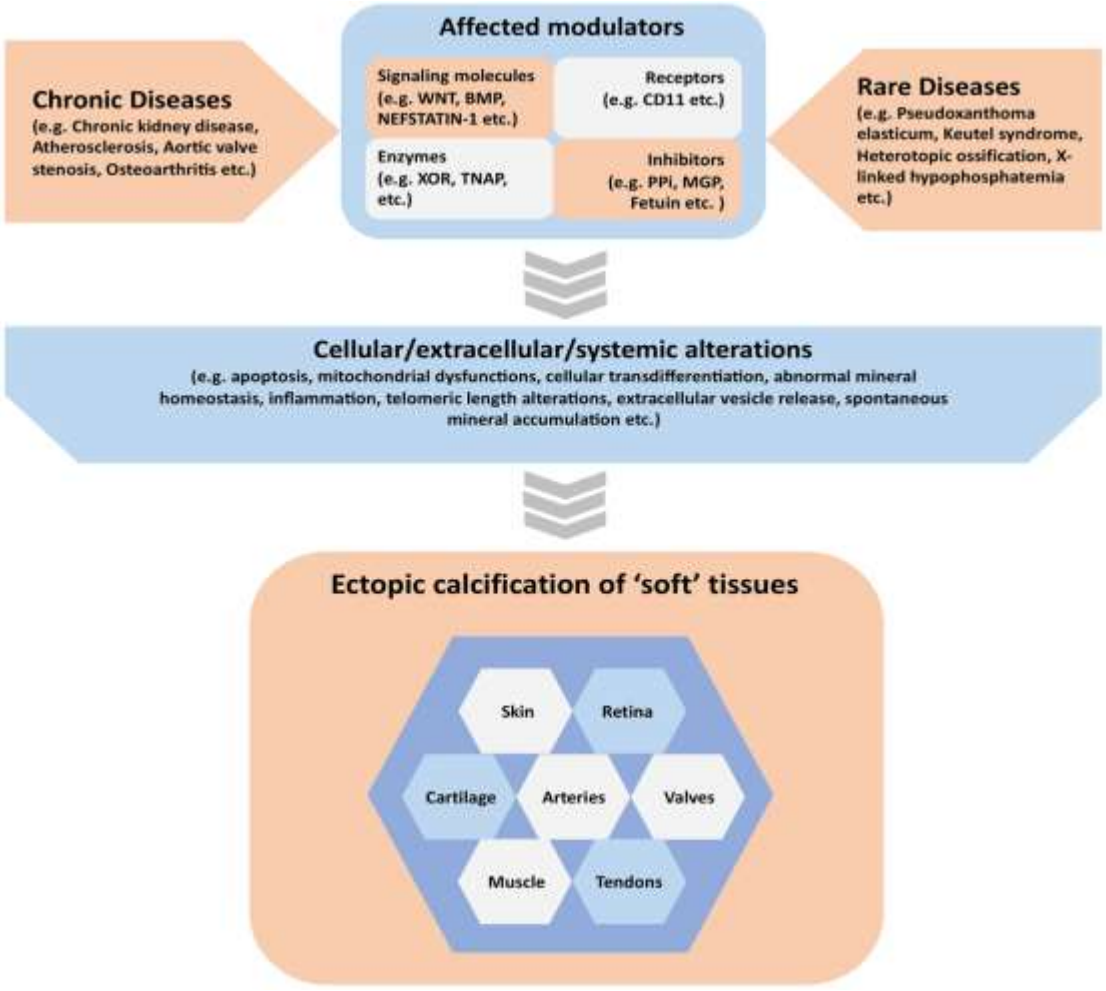

Figure D: Graphical summary of the contents covered in the manuscripts published in the special issue. Ectopic calcification in various "soft" tissues can be associated with both chronic and rare diseases. These diseases may affect one or more modulators of "soft" tissue calcification, which include but are not limited to signaling molecules, receptors, enzymes, and other proteins or inorganic molecules acting as mineralization inhibitors. These activating or inhibiting modulators may in turn alter a variety of cellular, extracellular, and systemic parameters in the extracellular matrix causing the initiation and progression of ectopic calcification in various "soft" tissues. Ref: Editorial: Ectopic Mineralization of tissues: Mechanisms, Risk Factors, Diseases, and Prevention Hervé Kempf 1*, Svetlana Komarova2,3 and Monzur Murshed2,3,4*

Figure E

Figure E: Schematic representation of the different domains of Matrix Gla Protein (MGP) structure. Gla residues indicated by blue dots and the Gla domain represented by blue box near the C-terminal. Phosphoserine residues are the green dots near the N-terminal and the domain is the green box. The proteolytic cleavage sites are indicated by red triangles, AxxF and RR. γ specifies the docking site for γ-glutamyl carboxylase. Circles containing 'C' letter represent conserved cysteine residues involved in the intramolecular disulfide bond. SP is the signal peptide. (Image from M.Cancela and V Laizé: From gene duplication to neofunctionalization Archives of Biochemistry and Biophysics, Volume 561,2014)

Figure F

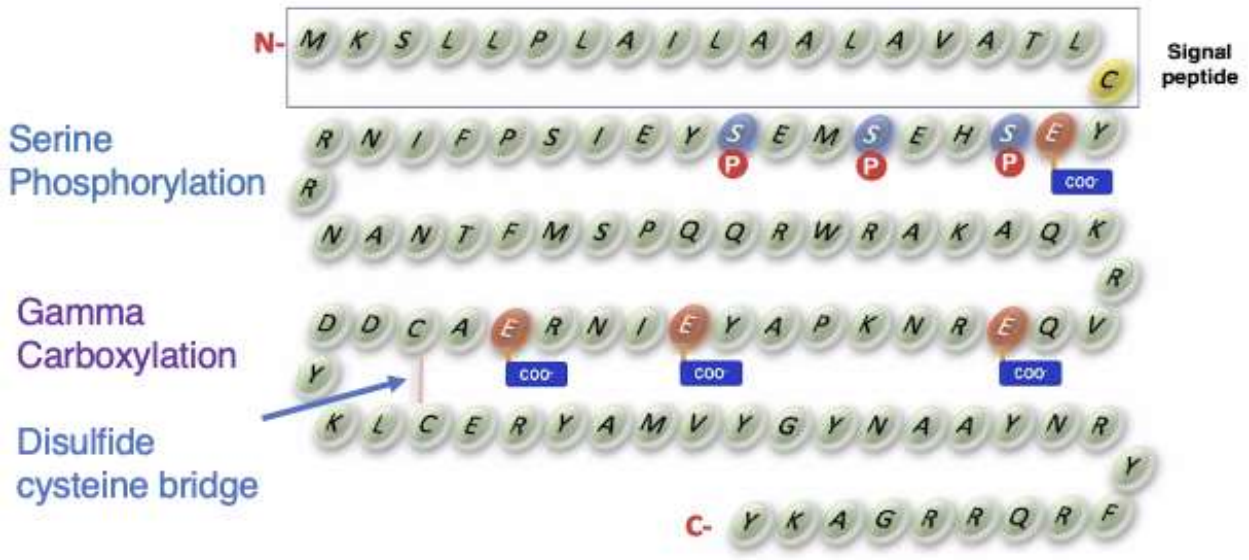

Figure F: Protein structure of MGP.MGP is a small (14 kDa) protein containing four conserved Glu residues, which undergo post-translational γ-carboxylation to form Gla (represented by the red molecules). Additionally, MGP undergoes post-translational phosphorylation of three conserved N-terminal serine residues (blue molecules). A disulfide cysteine bridge and signal peptide cleavage are the other known MGP's post-translation modifications (Images taken with permission from Dr. Murshed's lecture notes)

Figure G

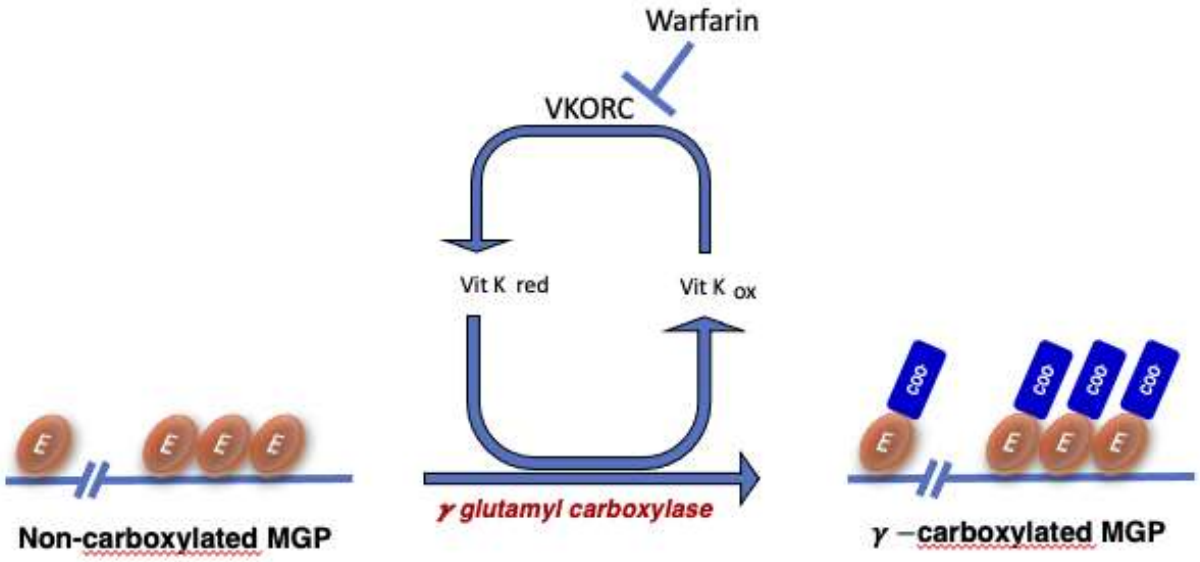

Figure G: Gamma carboxylation of glutamic acid residues: Schematic representation of MGP's gamma carboxylation. Four glutamic acid residues undergo gamma carboxylation by the help of gamma glutamyl carboxylase where reduced form of vitamin is required as a cofactor. Oxidation and reduction of vitamin k is acontinues process dependent on vitamin epoxide reductase (VKORC). Presence of Warfarin can inhibit this reaction.

Figure H

Figure H: Schematic presentation of the phosphorylation of serine residues in MGP. Three conserved serine residues undergo phosphorylation in the presence of an enzyme, unknown kinase.

Figure I

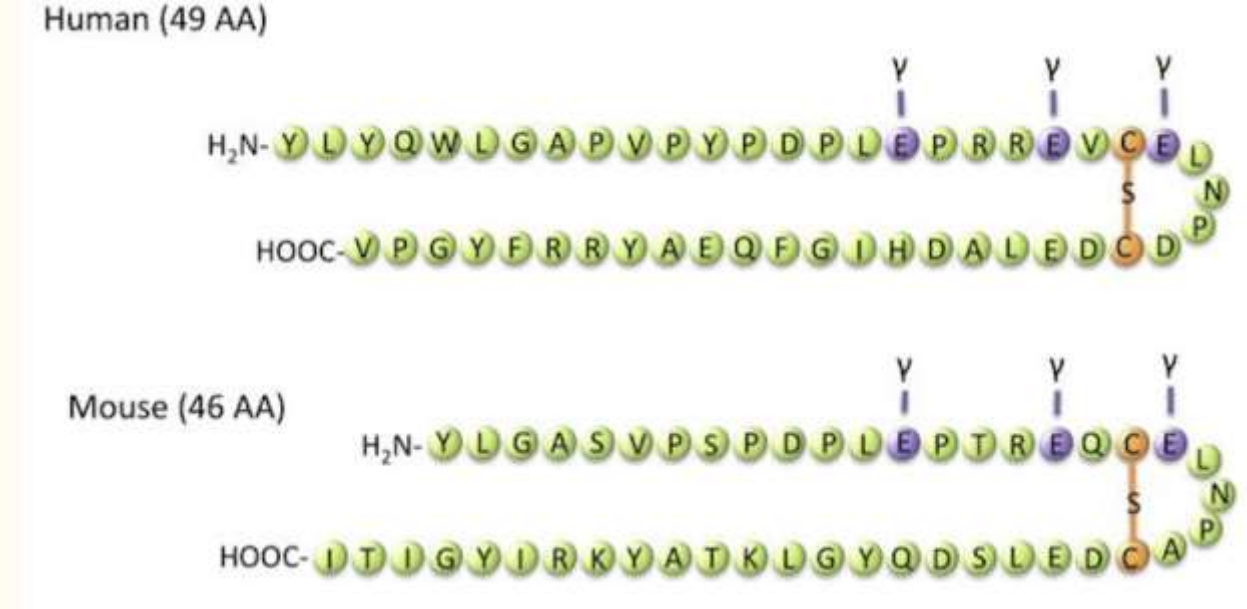

Figure I: The structure of osteocalcin (BGP) is marked by three γ-carboxyglutamic acid residues and a disulfide bond. The human protein contains 49 amino acids with γ-carboxyglutamic acid residues at positions 17, 21, and 24 and a disulfide bond between cysteine residues at positions 23 and 29. The mouse protein is 3 amino acids shorter with γ-carboxyglutamic acid residues at positions 13, 17, and 20.(Ref: New Insights into the Biology of Osteocalcin, Meredith L. Zoch, Thomas L. Clemens, and Ryan C. Riddle)

Chapter2: Objective

Overarching goal:

The overarching goal of this project is to determine whether the 3 conserved serine residues present at the N-terminal of MGP can confer anti-mineralization properties to BGP/osteocalcin, which, despite being a Gla protein like MGP, cannot prevent vascular calcification.

MGP is among the most potent mineralization inhibitors in vascular smooth muscle cells. Two Gla containing bone proteins (MGP and BGP) have a similar structure but do not show the same anti mineralization function. Whether or not MGP's conserved Gla and N-terminal phosphorylated serine residues both contribute to MGP's anti-minerlaization function is still a question that remains unanswered. To address this gap in knowledge, the current project is focused on the development of an in vivo model which expresses BGP, a Gla protein, in fusion with MGP's N terminal peptide carrying the serine residues. As mentioned in chapter1, vascular calcification may lead to death in certain patients with chronic kidney disease, atherosclerosis, generalized arterial calcification in infancy, etc. The new model expressing an MGP-BGP fusion protein in the blood vessels may help us understanding the mode of action of MGP, particularly its N-terminal serine residues in the prevention of vascular calcification.

My objective is to generate transgenic mouse lines which will express a chimeric MGP-BGP protein. In this protein, The N-terminal part of MGP carrying the serine residues will be fused to the mature BGP protein. The transgene expression will be driven by a *SM22α* promoter active in vascular smooth muscle cells (VSMCs). At least two founder lines will be generated and validated for VSMC-specific expression of the transgene. The transgenic mice will eventually be mated with *Mgp+/-* mice to achieve transgene expression on *Mgp-/-* background. The resultant mice will be analyzed by X-ray imaging and histological methods to examine the initiation and

progression of vascular calcification.

We expect that the MGP-BGP fusion protein will show anti-mineralization functions in the vascular tissues. If it does, it will suggest that adding the N-terminal MGP peptide sequence carrying the conserved serine residues is sufficient to confer anti-mineralization function to BGP. This initial finding will serve as a basis for future experiments to investigating how the conserved serine residues and their post-translational modification may affect ECM mineralization.

Specific Aims:

Objective I: Characterize and analyze MGP deficient *Mgp*$^{\Delta 55\text{-}62/\Delta 55\text{-}62}$ mouse line

Objective II: Generate transgene constructs to express modified BGP carrying MGP's serine residues.

Chapter3: Materials and Methods

Establishing*Mgp*$^{\Delta 55\text{-}62/\Delta 55\text{-}62}$mouse line:

We obtained the *Mgp*$^{+/\Delta 55\text{-}62}$mice by chance while screening for another mutation introduced by the CRISPR/CAS9 method. Upon sequence confirmation these mice were inbred and *Mgp*$^{\Delta 55\text{-}62/\Delta 55\text{-}62}$were generated at the animal facility of the Shriners Hospitals for Children, Montreal, Canada. For genotyping, tail biopsies were collected for DNA extraction and PCR was performed using primers C19Mgp$^{\Delta 55\text{-}62/\Delta 55\text{-}62}$/F and C19Mgp$^{\Delta 55\text{-}62/\Delta 55\text{-}62}$/R (see supplemental Table I) and purified by using QIAquick Gel Extraction Kit Protocol. Sanger sequencing was performed at Genome Quebec using the Nanuq platform and sequences were analyzed by the DNA Strider software.

PCR for *Mgp*$^{\Delta 55\text{-}62/\Delta 55\text{-}62}$ *mice*:

For a direct PCR-based genotyping without (DNA sequencing), two forward primers were designed which ended with a specific nucleotide to specifically anneal at the wild type or the mutated allele (C for wild type and A for the mutated allele). The usability of the primers was first confirmed by gradient PCRs using one of the forward primers and a common downstream reverse primer which identified the suitable annealing temperatures (62°C for wild type and 60°C for the mutant allele). Both the PCR generated amplicons of 700 base pairs. The sequences of the primers were Mgp$^{\Delta 55\text{-}62/\Delta 55\text{-}62}$/F. wild and Mgp$^{\Delta 55\text{-}62/\Delta 55\text{-}62}$/R for the wild type allele and LY- Mgp$^{\Delta 55\text{-}62/\Delta 55\text{-}62}$/F andMgp$^{\Delta 55\text{-}62/\Delta 55\text{-}62}$/R for the mutated allele are presented in table I. PCR condition: Denaturation at 94°C for2min, annealing at 62°C or 60°C for30sec, and elongation at 72°C for7min.

Dissection of the skeleton:

The control and*Mgp*$^{\Delta 55\text{-}62/\Delta 55\text{-}62}$ mice were euthanized. The skin, internal organs and the muscles were removed as much as possible. The skeleton was kept in buffered formalin (Fisher) for overnight and kept in 70% Ethanol for further experiments.

Radiography:

The x-ray images were taken by using high-resolution radiography, under identical conditions by using a KUBTEC XPERT-80 radiography system; manufacturer: KUB Technologies Inc. (Milford, CT). Specifications: Geometric magnification of 1- 5X with 5–45-micron focal spot; energy range: 10-90 kV; tube current: up to 1.0 mA; detector size: 10 cm X 10 cm (4"x 4"); power settings used for the project: 21.5kV/570uA.

Staining of thoracic aorta by alcian blue and alizarin red:

Thoracic part of the skeletons with the aortas was dissected out of the whole skeleton (kept in 70% ethanol as described above) and was transferred to 95% ethanol for overnight. The samples were then stained in 0.015% alcian blue dye (Sigma-Aldrich) and put back in 95% ethanol for 3 hours and transferred to 2% KOH for 24 hours. The samples were then stained overnight in alizarin red solution (0.005%Alizarin sodium sulphate in 1% KOH). The skeletons were cleared in 1% KOH/20% glycerol for at least 2 days and stored in a 1:1 mixture of glycerol and 95% ethanol.

Plastic embedding and histological staining of the thoracic aorta:

Small pieces of thoracic aorta attached to the thoracic vertebrae from the control or mutant mice

were placed in a plastic cassette and placed in 100% ethanol for 24 hrs at 4°C(2X), transferred to Xylene for 4 hrs at room temperature and then placed in solution I(60 ml of methyl methacrylate,30 ml butyl methacrylate,5 ml methyl benzoate and 1.2 ml PEG)for 24 hours in 4°C. Next, the sample cassettes were transferred to solution II (Sol.I and 0.5g of benzyl peroxide; BPO) for 24 hours in 4°C. For embedding, fresh solution I was prepared and 0.8 g of BPO was added and stirred for 1 hr. Next 600 microliter of N-N-Dimethyl p-toluidine (DMPT) was added and stirred for another 7-8 minutes. The samples were taken out of the cassette and placed it in the glass vials with proper orientation. The embedding solution was added carefully; vials were capped and placed in an ice chamber at4°C for 48 hours. The embedded samples were cut using a rotary microtome (Leica) at 7-micron thickness.

Von Kossa and Van Gieson (VKVG) staining:

The plastic sections on glass slides were deplasticized in 1-acetoxy-2-methoxy-ethane for half an hour and stained by the method described by von Kossa (to detect minerals) and van Gieson (to detect collagen) (VKVG). Briefly, samples were serially hydrated, stained with silver nitrate, treated with sodium thiosulfate and sodium formamide and stained by van Gieson. Dehydrated samples were mounted using a xylene-based mounting solution. Images were taken using a light microscope (DM200; Leica Microsystems) with 20X (with numerical aperture of 0.40)and 40X (numerical aperture of 0.65)objectives. All histological images were captured using a digital camera (DP72; Olympus Canada Inc), acquired with DP2-BSW software (XV3.0; Olympus Canada Inc) and processed using Photoshop software (Adobe).

Table I (Sequences of primers for *Mgp*$^{\Delta 55\text{-}62/\Delta 55\text{-}62}$ mice):

Primers Name	Primers sequence for *Mgp*$^{\Delta 55\text{-}62/\Delta 55\text{-}62}$ mice
LY- Mgp$^{\Delta 55\text{-}62/\Delta 55\text{-}62}$ /F	5'GCCGTGGCAACCCTGTGA3'
LY- Mgp$^{\Delta 55\text{-}62/\Delta 55\text{-}62}$ /R	5'CATGCTTTCGTGAGATTCGTAT3'
Mgp$^{\Delta 55\text{-}62/\Delta 55\text{-}62}$ /F_wild	5'GCCGTGGCAACCCTGTGC 3'
Mgp$^{\Delta 55\text{-}62/\Delta 55\text{-}62}$ /R	5'CGAGAGGCATAACATTAGAGC3'
C19 Mgp$^{\Delta 55\text{-}62/\Delta 55\text{-}62}$ /F	5'GGCAAGTTTAGTGCCAAGC 3'
C19 Mgp$^{\Delta 55\text{-}62/\Delta 55\text{-}62}$ /R	5'ACATGCGCTGGAATGACAATG'3

DNA Construct and plasmid generation:

***pSM22αMBgp-1 and -2* Transgene model DNA construct:**

We generated DNA construct for the *pSM22αMBgp-1 or -2* transgenic models. In this project we are interested in studying the role of serine residues of *Mgp* in vascular tissues. For that we used the *pCTFMgp, pBgp, pSV40, pβ-globulin intron* and *pSM22αMgp* plasmids from our lab. We wanted to introduce EcoRV restriction site in the N-terminal part of *Mgp* coding sequence. The codon table's application (https://en.wikipedia.org/wiki/DNA_and_RNA_codon_tables) was used to design the primers. The primer sequences were 5' GAT ATC TCC CTT CAT CAA CAG 3' and 5'TCA TAG GAC TCC ATG CTT TCG 3' with having the desired mutation AATCAG(MGP)>GATATC(EcoRV)). For introducing EcoRV site we used the Q5® Site-Directed Mutagenesis Kit (New England Biolabs, Catalog number E0554S). This kit works by using polymerize chain reaction method and individually predesigned back-to-back primer set to substitute the sequence to the desired ones. Our template DNA was *pCTFMgp*. First, we did PCR of *pCTFMgp* and treated with KLD for 5 minutes in room temperature to get rid of the template DNA, phosphorylate the 5' end and ligate both ends. Then the circular plasmid was transformed into high-efficiency NEB 5-alpha Competent E-coli (New England Biolabs). After transformation we did mini and midi followed by Invitrogen protocol (Thermo Fisher Scientific Kit). Finally we confirmed the plasmid *pCTFEoVMgp* by Sanger sequencing result. The second insertion was *Bgp* full length coding sequence. We used *pBgp* plasmid from lab and designed primers to amplify *Bgp* coding sequence (pro-peptide and mature peptide).The forward Bgp primer designed in a way to introduce 5 nucleotides of Mgp (ATCTC) sequence at the 5' end of the primer and added rest of the nucleotides from *Bgp* ORF(Bgp-Forward-Table II**)** and we

designed the reverse primer from the reverse strand of *Bgp* ORF(Bgp-Reverse-Table II**)**.By using these primers we did PCR(Q5 high enhancer kit) of *pBgp* to amplify the *Bgp* coding sequence. The amplified PCR product run on1% agarose gel and purified the PCR products with QIAquick Gel Extraction Kit (Qiagen, Catalog number 28704) and also did PNK treatment. The *pCTFEcoVMgp* digested with EcoRV and kept 2 ½ hours in 37° incubator and did CIP treatment. Finally, we set up ligation with ligation kit (Biolab-(M2200S) and did transformation followed by above protocol. Finally, the Sanger sequencing result confirmed the plasmid *pCTFEMBgp*. For the insertion of rest of the fragments of *pSM22αMBgp-1* transgene we designed a double stranded DNA linker by adding some restriction enzymes SpeI, BglII, XbaI, BamHI and also ordered the linker (sequences of linker are presented in Table II). Then we took the plasmid *pβ-globulin intron* from lab for insertion of DNA Linker. *pβ-globulin intron* digested with NotI and XbaI and did CIP treatment. In the meantime, we also did kinase treatment of DNA Linker by PNK. Finally, set up ligation with same competent cells and did transformation and sent for sequencing to confirm that DNA linker inserted into *pβ-globulin intron* (*pβ-Linker*). Next, we inserted *SV40* in the plasmid*pβ-Linker.*We took *pSV40* plasmid from lab digested with BamHI and *pβ-Linker* also digested with XbaI and finally, we got*β-Linker-SV40*.

Next, we amplified MGP-BGP fusion sequence from the plasmid (*pCTFECoVMBgp*). Though the Flag sequence (DYKDDDDK) present in this plasmid. So, we designed forward primer by removing this flag sequence and added SpeI (ACTAGT) nucleotides and 3A (AAA) nucleotides at the 5'end of the primer from *Mgp* ORF(Spe-MgpORF5'/F) and also designed reverse primer by adding BglII (AGATCT) nucleotides at the 5'end of the primer from *Bgp* ORF(BglII-BgpORF3'/R) are presented in table II. By using those primers we did PCR(Q5 high fidelity

Kit)of *pCTFECoVMBgp*. After purification of the PCR product, we did double digestion with SpeI and BglII. In the meantime, we digested *pβ-Linker-SV40*with SpeI and BglII. Finally, we set up ligation and transformation by using same cloning protocol as we did before and got the plasmid*pβ-MBgp-SV40*. The final part was to insert of *SM22α*promoter in the plasmid (*pβ-MBgp-SV40*). We took *pSM22αMgp* plasmid from lab and digested with XhoI and also digested *pβ-MBgp-SV40*with XhoI. Finally, we got first transgene construct *pSM22αMBgp-1*.

After constructed of *pSM22αMBgp-1* transgene, we generated a second construct (*pSM22αMBgp-2*). In the second construct we amplified the BGP coding sequence; translate only for mature protein from *pBgp*. First, we designed the forward primer (Bgp/F; Table II) by using only mature BGP protein sequence and added 5 nucleotides of MGP (ATCTC) at the 5' end of *Bgp* ORF. We used reverse primer as we designed in first construct (Bgp -Reverse; Table II) and did PCR of *pBgp* plasmid and inserted into the plasmid *pCTFECoVMg*p which we already made in our first construct and got *pCTFECoVMBgp*. Then we did PCR of the plasmid (*pCTFECoVMBgp*) to amplify MGP-BGP fusion sequence by using the primers (Spe-MgpORF5'/F, BglII-BgpORF3'/R; are presented in Table II) and inserted this fusion sequence into the*pβ-Linker-SV40* vector. The resultant vector was named as*pβ-MBgp-SV40*.The last step was to insert *pSM22α* promoter by following the same procedure as we did in first construct, and we got the second construct *pSM22αMBgp-2*.

For the final confirmation of experiment of both*pSM22αMBgp-1&2* transgenes, we digested *pSM22αMBgp-1 &2* with XhoI, BglII and BamHI and incubated in 37° incubator for 2 hours and ran on 1% agarose slow run gel. From the images of gel we confirmed the insertion of all

fragments of transgenes by the band size of each DNA fragment. We used kb-plus ladder as a maker for measuring the band sizes.

Table II (Sequences of Primers for cloning of*pSM22αMBgp-1&2* transgene)

Name of the primers	Primers for cloning
Mgp-EcoV_Forward	5' GAT ATC TCC CTT CAT CAA CAG 3'
Mgp_Reverse	5' TCA TAG GAC TCC ATG CTT TCG3'
Bgp-Forward	5'ATC TCC CAT GAG GAC CCT C 3'
Bgp-Reverse	5' AAT AGT GAT ACC GTA GAT GCG 3'
Spe-MgpORF5'/F	5'AAAACTAGTATGAAGAGCCTGCTCC 3'
BglII-BgpORF3'/R	5' AGGAGATCTAAATAGTGATACCGTAG 3'
SPE-SBXB-NOT/F:	5'CTAGTTAGTAAAACTAGTAAAAGATCTAAATCTA GAAAAGGATCCAAAGGCCGCGC 3'
NOT-BXBS-SPE/R	5'GCCGCGCGGCCTTTGGATCCTTTTCTAGATTTAG ATCTTTTACTAGTTTTACTAA 3'
Bgp /F(2ndTransgene)	5' ATCTCTACCTTGGAGCCTCAGTCC'3

Study approval:

All animal experiments were performed according to Animal Use protocol 7132, approved by the Animal Care Committee of McGill University.

Chapter4: Results

Establishment of an in-vivo model of MGP deficiency: The *$Mgp^{\Delta 55\text{-}62/\Delta 55\text{-}62}$* mouse line

We obtained a male *$Mgp^{+/\Delta 55\text{-}62}$* mouse while screening for another mutation in the 5' open reading frame of *Mgp* gene generated by a CRISPR/Cas9-based genome editing approach (**Figure 1**). Although a template ssODN carrying the desired mutation was co-injected together with the gRNA and Cas9 complex into the fertilized ova, we found an unexpected presence of a Δ55-62 mutation in the sequenced PCR products obtained from the genomic DNA (**Figure 2**). The chromatogram showed the presence of overlapping bands starting from nucleotide 57(**Figure 2**).

We next mated the *$Mgp^{+/\Delta 55\text{-}62}$* mouse with a wild type (*$Mgp^{+/+}$*) female mouse to generate more *$Mgp^{+/\Delta 55\text{-}62}$* mice. The *$Mgp^{+/\Delta 55\text{-}62}$* mice were inbred to generate *$Mgp^{\Delta 55\text{-}62/\Delta 55\text{-}62}$* mice in the F2 generation (**Figure 3**). These homozygous mice were used for further analyses.

DNA isolated from the tail biopsies of the mice obtained in the F2 generation were PCR amplified using *Mgp* locus-specific primers flanking the identified site of mutation. The PCR resulted in a 700 base pair band (**Figure 4A**), which was then sequenced. The sequencing revealed the presence of wild type and heterozygous mice, as well as mice homozygous for the mutation. A further comparison of the *Mgp* sequence of the homozygous mutant mouse to that of wild type mouse revealed a deletion of 8 nucleotides (**Figure 4B and C**).

The *$Mgp^{\Delta 55\text{-}62/\Delta 55\text{-}62}$* mice were smaller as *$Mgp^{-/-}$* mice as reported earlier [Luo et al Nature, 1997]. Dissected skeletons of the *$Mgp^{\Delta 55\text{-}62/\Delta 55\text{-}62}$* mice at 6 weeks of age were markedly shorter than control wild type (*$Mgp^{+/+}$*) skeletons as demonstrated by the photographic and X-ray images

(**Figure 5**).

Massive Vascular calcification is a hallmark of *Mgp*$^{-/-}$ mice. We next examined whether this trait is present in our newly generated *Mgp*$^{\Delta 55\text{-}62/\Delta 55\text{-}62}$mice. Alcian blue and alizarin red staining of the thoracic skeleton with the aorta attached demonstrated the presence of calcified arteries in 6-week-old*Mgp*$^{\Delta 55\text{-}62/\Delta 55\text{-}62}$mice, but not in the sex-matched control mice (**Figure 6A**). This finding was further confirmed by histological staining. Thin plastic aorta sections from 6-week-old control and *Mgp*$^{\Delta 55\text{-}62/\Delta 55\text{-}62}$mice were stained by von Kossa (stains phosphate minerals in black) and van Gieson (stains collagen in pink). As presented in (**Figure 6B)**, mineral deposition was found along the elastic lamina in *Mgp*$^{\Delta 55\text{-}62/\Delta 55\text{-}62}$ mice, as previously reported in *Mgp*$^{-/-}$mice [70]. No mineral deposition was found in the control aortas.

For a direct PCR-based genotyping without (DNA sequencing), two forward primers were designed which ended with a specific nucleotide to specifically anneal at the wild type or the mutated allele (C for wild type and A for the mutated allele) The usability of the primers were first confirmed by gradient PCRs using one of the forward primers and a common downstream reverse primer which identified the suitable annealing temperatures. Both the PCR generated amplicons of 700 base pairs. From the images of the gel, we confirmed the wild type of PCR (*Mgp*$^{+/+}$) and mutant PCR (*Mgp*$^{\Delta 55\text{-}62/\Delta 55\text{-}62}$) (**Figure 7**).

Generation of DNA constructs to produce transgenic models to study the function of MGP's N'-terminal peptide

We intended to express a fusion protein with MGP's N-terminal peptide (YESHESMESYEISP) linked in frame to the N terminal end of the native or cleaved BGP/osteocalcin sequence in the VSMCs of our new MGP-deficient mice. The transgene constructs *pSM22αMBgp1* (coding for the full-length BGP sequence), or *pSM22αMBgp2* (coding for the BGP sequence after propeptide cleavage) carries the *SM22* promoter to drive VSMC-specific expression of the transgene. A rabbit *β-globulin* intron has been added after the promoter, which is followed by the MGP-BGP coding sequence preceded by a Kozak sequence for the initiation of translation. A stop codon is present at the 3' end of the coding sequence to terminate translation. The protein coding sequence is followed by a SV40 polyadenylation signal for the termination of transcription. A step-by-step description of transgene generation is given below.

For generating the *pSM22αMBgp-1* transgene model:

First step was introduced an EcoRV site in the existing *pCTFMgp*DNA construct. A PCR-based approach was pursued in a way that the introduction of a novel EcoRV site in the DNA sequence did not alter the amino acid sequence. The back-to-back forward (Mgp-EcoV_Forward; see Table II) and reverse primers (Mgp_Reverse; see Table II) were designed following the guidance provided by the Q5® Site Directed Mutagenesis Kit. This kit first generates linearized PCR products carrying the desired mutation, which is then phosphorylated and ligated by the enzymes provided by the supplier. Simultaneously, the enzymatic process removed the original template plasmid. The newly generated plasmid was propagated by transformation of competent bacteria. The resultant plasmid was named as *pCTFEcoVMgp* (**Figure 8 Step I**).

In the second step, *Bgp* sequence (coding for the full-length *Bgp* pro-peptide or the processed peptide after cleavage) was PCR amplified from an existing *pBgp* construct. We designed the forward primer (*Bgp*-Forward) in a way that it carries 5 nucleotides from the *Mgp* coding sequence (ATCTC) atits5'end, while the rest of the nucleotides were from the5' end of the *Bgp* cDNA. The reverse primer (*Bgp*-Reverse) carried the complementary sequence to the 3' end of *Bgp* including the stop codon (See Table II for the primer sequences). The purified PCR products were digested with EcoRV, treated by polynucleotide kinase (PNK) to phosphorylate and ligated to EcoRV-digested, dephosphorylated (by calf-intestinal phosphatase; CIP) *pCTFEcoVMgp*. Sanger sequencing was performed to confirm that desired *Bgp* sequence was inserted into the *pCTFEcoVMgp* vector. The resultant vector was named as *pCTFEMBgp* (**Figure 8 step2**).

The third step was to make an artificial double stranded DNA linker for insertion of rest of the transgene fragment in the existing *pβ-globulin intron*. We took *pβ-globulin intron* from our lab for insertion of DNA linkers. *pβ-globulin intron* digested with NotI and XbaI and Linker also treated with PNK (Poly nucleotide kinase) to make phosphorylated. Finally, we confirmed the DNA linker added with beta globulin intron by sending for Sanger sequencing and we got the new plasmid *pβ-Linker* (**Figure8 Step 3**).

The fourth step was to insert of *SV40* in the plasmid (*pβ-Linker*). we took *pSV40*plasmid from lab and digested with BamHI and *pβ-Linker* also digested with XbaI. Finally, we got *pβ-Linker-SV40* (**Figure8 Step4**).

The fifth step was amplification of *Mgp-Bgp* fusion fragments from the plasmid (*pCTFEMBgp*). By using the primers (Spe-MgpORF5'/F andBglII-BgpORF3'/R; present in Table II), we did PCR of *pCTFEMBgp*. The purified PCR product was digested with SpeI and BglII. In the meantime, we digested *pβ-Linker-SV40* with SpeI and BglII. At the end we got the plasmid (*pβ-MBgp-SV40*) (**Figure 8 Step 5**).

The final step was insertion of *SM22α* promoter in the plasmid (*pβ-MBgp-SV40*). We took *pSM22αMgp* plasmid from our lab and digested with XhoI and *pβ-MBgp-SV40*also digested with XhoI. Finally, we confirmed the full transgene construct*pSM22αMBgp-1* (1st Transgene) by Sanger sequence result (**Figure8 Step 6 and Figure 9**).

After generating of 1st transgene, we figured out that though we took BGP propeptide and mature peptide, there was a cleavage site in between 2 peptides. So, when we will express this transgene there will be a chance of loss of mature BGP protein due to the presence of cleavage site. For this reason, we generated a second construct of transgene which contains only mature BGP protein.

For generating the *pSM22αMBgp-2* transgene model:

First, we amplified the BGP mature protein from the existing plasmid(*pBgp*) by PCR and inserted into the plasmid(*pCTFECoVMgp*) which we made in first transgene construct, and we obtained the plasmid (*pCTFECoVMBgp*). Then this plasmid we did PCR for amplifying the *Mgp-Bgp* sequence by using the same primers (Spe-MgpORF5'/F, BglII-BgpORF3'/R) as we used in first transgene. Then the purified PCR product was digested with SpeI and BglII and *pβ-*

*Linker-SV40*digested with SpeI and BglII. Finally, we got the *pβ-MBgp-SV40*.Then we again inserted *SM22α*promoter in*pβ-MBgp-SV40,* followed the same procedures as we did in first transgene construct and finally, we got the second construct *pSM22αMBgp-2* (**Figure 8 and Figure 9).**

At the end we confirmed both transgenes by digestion with XhoI, BglII and BamHI and got the desired band sizes of all fragments (*pSM22αMBgp-1 &2*) which we inserted into the DNA construct after running on gel (**Figure 9 and Figure 10**).

Figures:

Figure 1

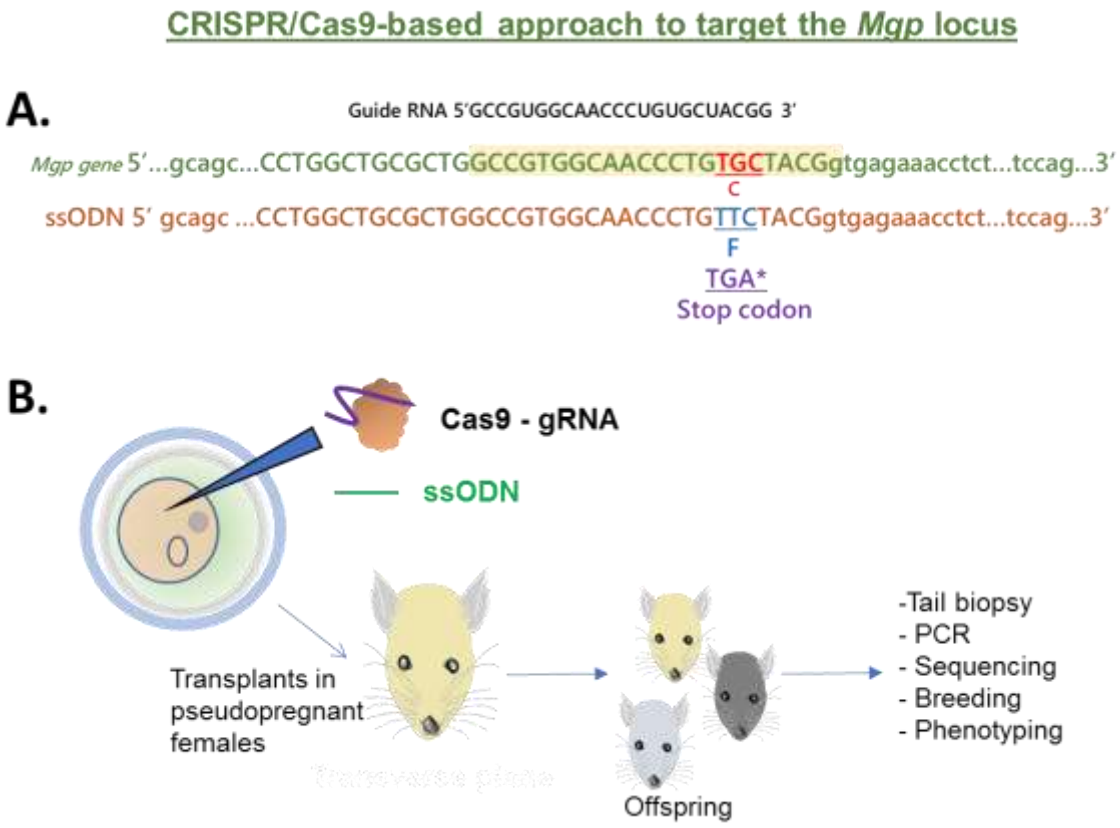

Figure 1: Introduction of mutation in the Mgp locus. A. The guide RNA and ssODN sequence to target the *Mgp* locus. The homologous guide RNA sequence in the gene sequence is highlighted. *Note: Although the strategy was intended to introduce the 56 G>T mutation, we obtained a mouse with a deletion mutation resulting in a premature stop codon (TGA) within the open reading frame. **B.** The methods used to target *Mgp* locus using the CRISPR/Cas9 approach. The steps followed to characterize the $Mgp^{\Delta 55\text{-}62/\Delta 55\text{-}62}$mice have been indicated.

Figure 2

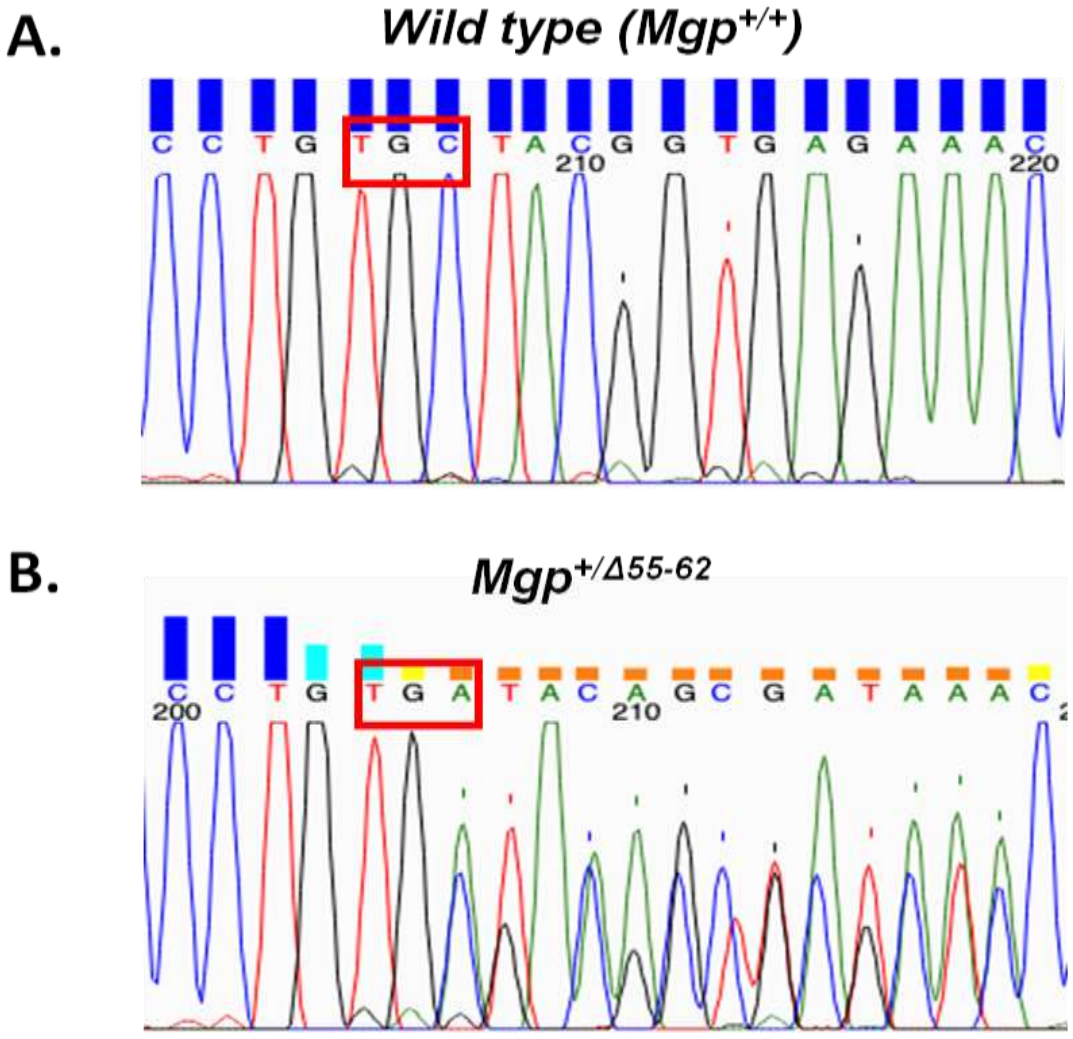

Figure 2: Identification of a nonsense mutation in *Mgp*.A. Sanger sequencing of the PCR products generated from wild type DNA sample. The cys19 codon TGC is shown in the red box. **B**. Sanger sequencing of the PCR products generated from a heterozygote mouse (named as *Mgp*$^{+/\Delta 55\text{-}62}$based on the deletion identified in the sequence of homozygote mice; see in Figure 4) showing the overlapping nucleotide peaks indicating the presence of 'indels'. Note that the cys19 codon is converted to the stop codon TGA (shown in red box).

Figure 3

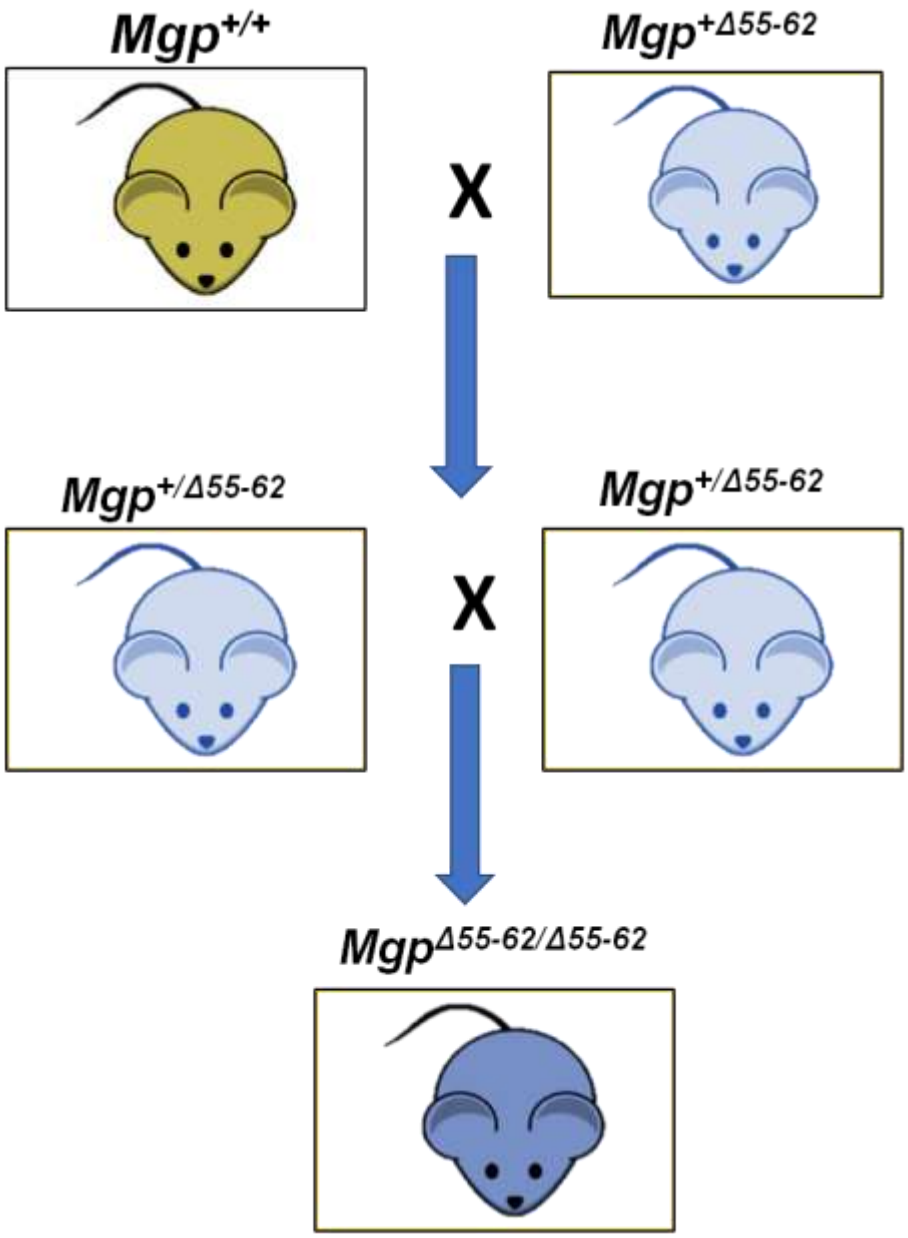

Figure 3: Breeding strategy to generate $Mgp^{\Delta 55\text{-}62/\Delta 55\text{-}62}$ mice: The founder $Mgp^{+/\Delta 55\text{-}62}$ mouse was first mated with a wild type ($Mgp^{+/+}$) mouse. The resultant $Mgp^{+/\Delta 55\text{-}62}$ mice were inbred to generate the $Mgp^{\Delta 55\text{-}62/\Delta 55\text{-}62}$ mice.

Figure 4

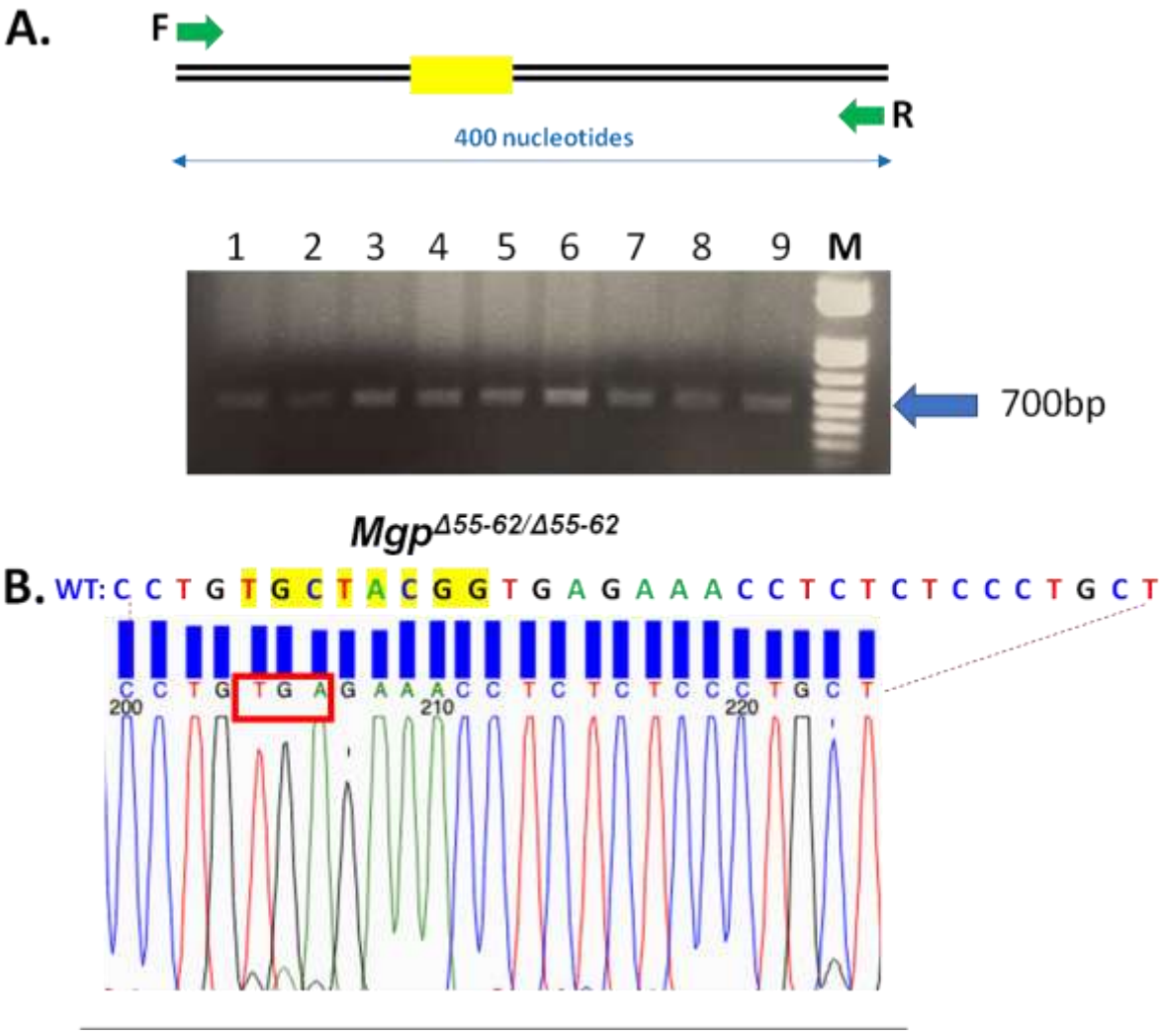

Figure 4: Analysis of *Mgp* sequence alterations. A. Upper panel: Schematic representation of a part of the *Mgp* gene showing the PCR primer (green arrows) annealing sites and the altered sequence (yellow box). Lower panel: Agarose gel electrophoresis of the PCR products generated from the tail biopsies from offspring of a heterozygote breeding (see Figure 3). **B.**Sanger sequencing confirmed the deletion of 8 nucleotides (TGCTACGG; highlighted in yellow in the WT sequence) in a homozygous (*Mgp*$^{\Delta 55\text{-}62/\Delta 55\text{-}62}$) mouse. This deletion replaces the original cystine 19 codon by a stop codon (Red box).

Figure 5

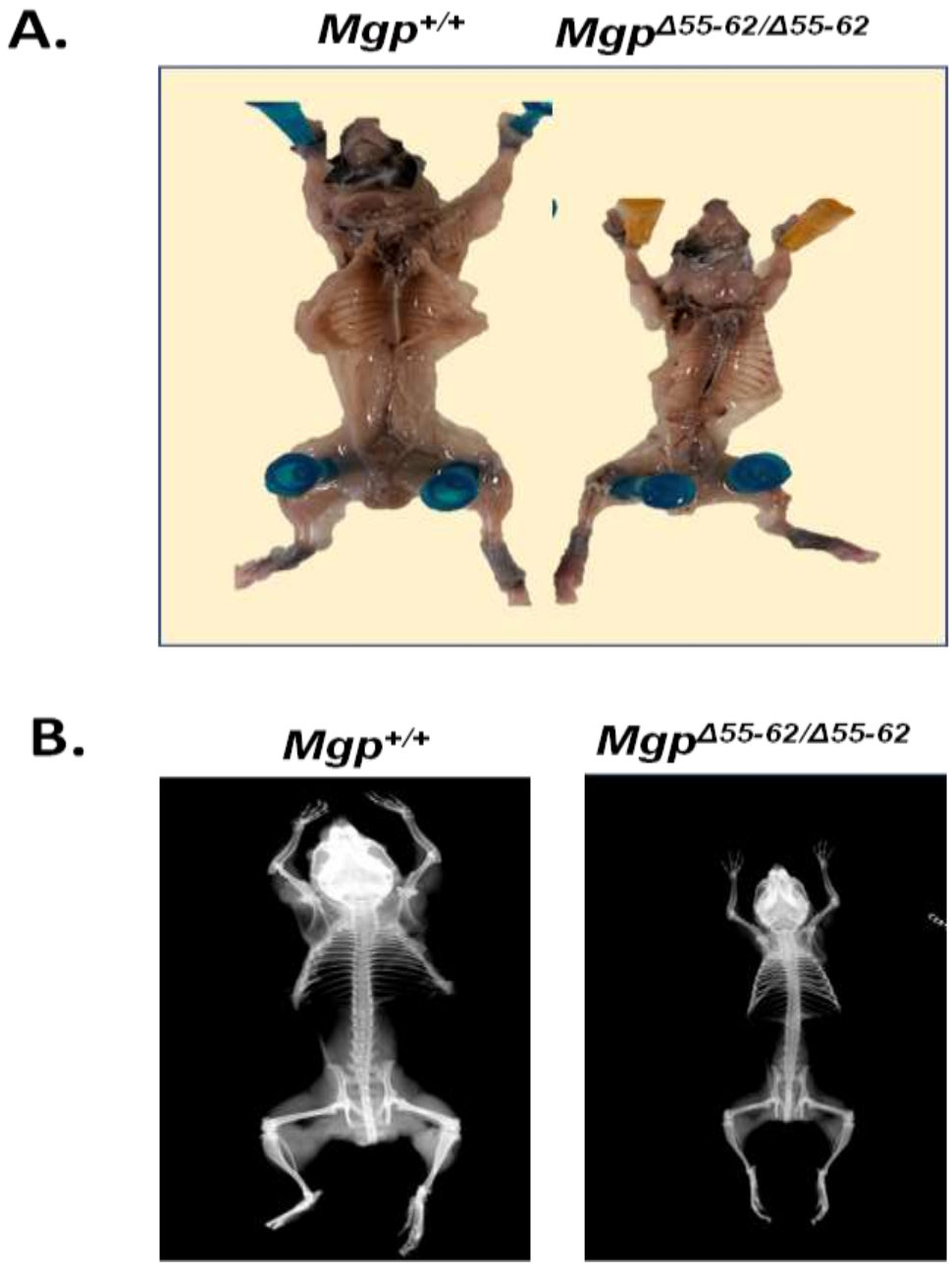

Figure 5: Skeletal analyses of *Mgp*$^{\Delta 55\text{-}62/\Delta 55\text{-}62}$mice.A. and **B.** Dissected skeletons and X-ray imaging showing the smaller size of *Mgp*$^{\Delta 55\text{-}62/\Delta 55\text{-}62}$mice, in comparison to the control wild type (*Mgp*$^{+/+}$) mice.

Figure 6

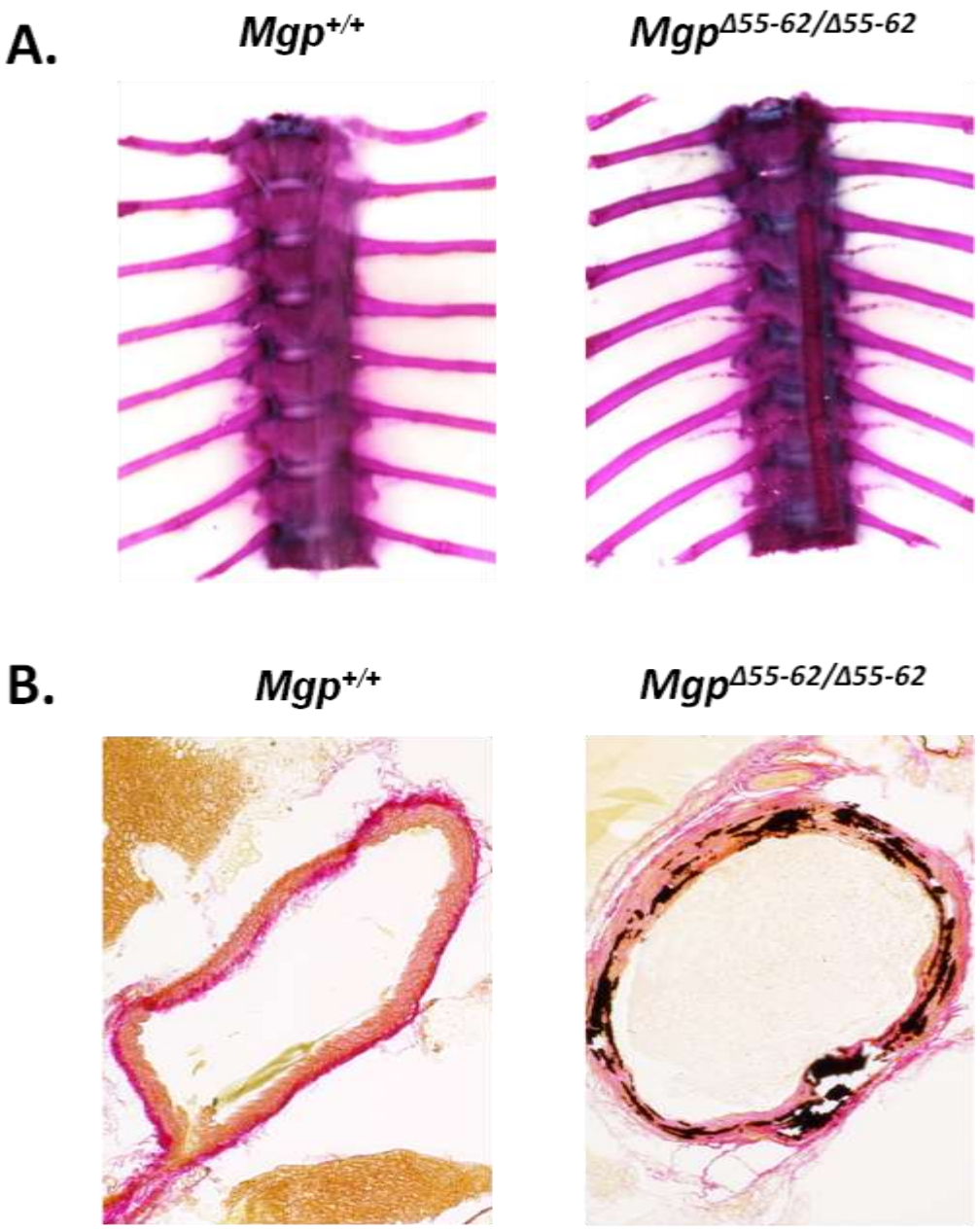

Figure 6: Analyses of arterial calcification in*Mgp*$^{\Delta 55\text{-}62/\Delta 55\text{-}62}$mice.A. Alizarin red staining of the thoracic skeleton shows calcified aorta in *Mgp*$^{\Delta 55\text{-}62/\Delta 55\text{-}62}$, but not in wild type (*Mgp*$^{+/+}$) mice **B.** Von kossa-van Gieson (VKVG) staining of the histological section of thoracic aorta of an *Mgp*$^{\Delta 55\text{-}62/\Delta 55\text{-}62}$mouse confirms calcific deposits (black) in the medial layer. No such staining detected in the wild type aorta

Figure 7

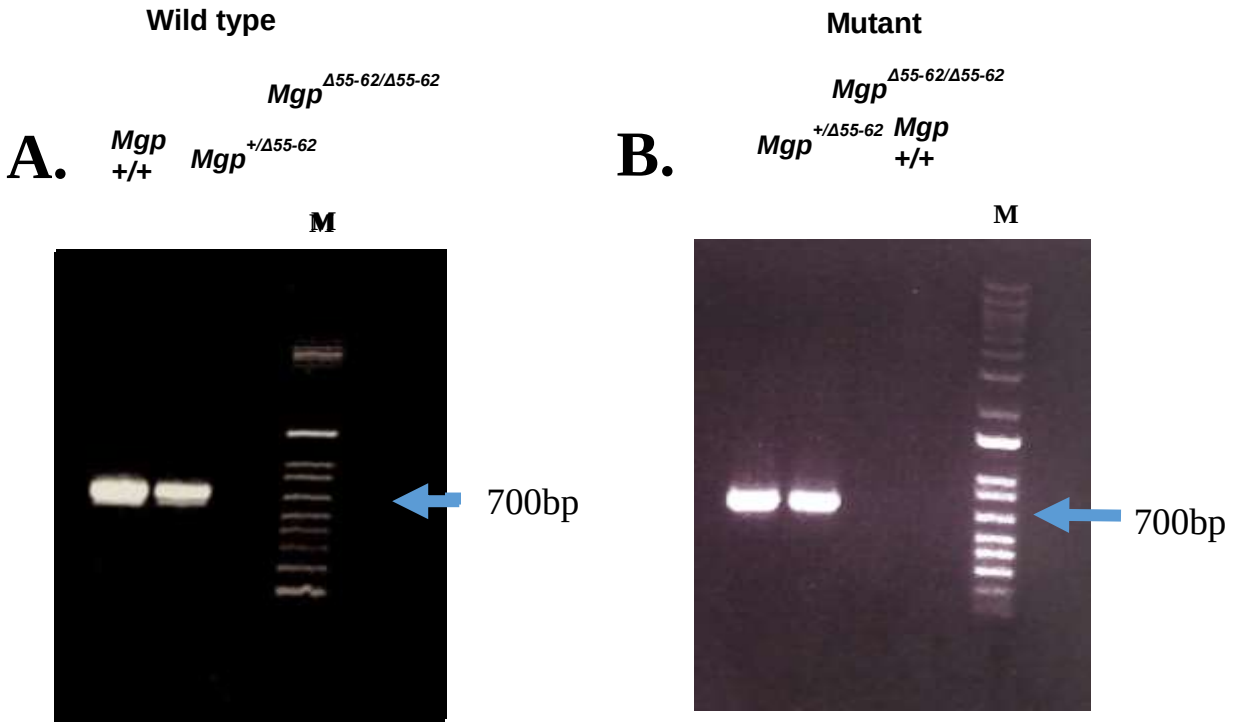

Figure 7: PCR genotyping to detect the mutated *Mgp* allele. Two forward primers were designed carrying a C (to detect the wild type allele) or an A (to detect the mutant allele) at the 3' end. Separate PCRs were performed with a common reverse primer. **A.** Ethidium bromide-stained agarose gel showing products of the wild type PCR on genomic DNA samples from $Mgp^{+/+}$, $Mgp^{+/\Delta 55\text{-}62}$, and $Mgp^{\Delta 55\text{-}62/\Delta 55\text{-}62}$ mice. **B.** Ethidium bromide-stained agarose gel showing products of the mutant PCR on genomic DNA samples from $Mgp^{+/\Delta 55\text{-}62}$, $Mgp^{\Delta 55\text{-}62/\Delta 55\text{-}62}$, and $Mgp^{+/+}$ mice.

Figure 8

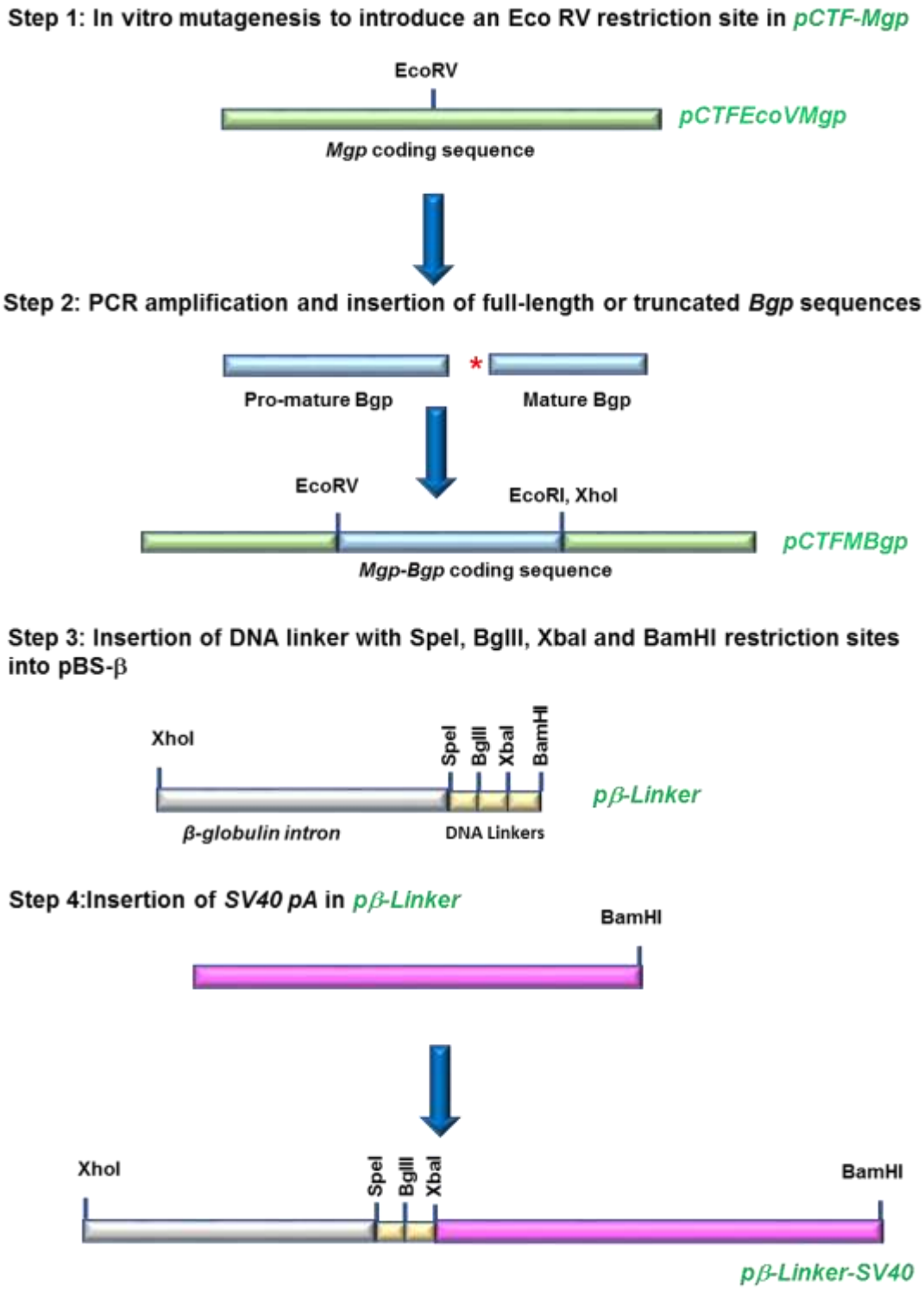
Step 1: In vitro mutagenesis to introduce an Eco RV restriction site in pCTF-Mgp
EcoRV
pCTFEcoVMgp
Mgp coding sequence
Step 2: PCR amplification and insertion of full-length or truncated Bgp sequences
*
Pro-mature Bgp
Mature Bgp
EcoRV
EcoRI, XhoI
pCTFMBgp
Mgp-Bgp coding sequence
Step 3: Insertion of DNA linker with SpeI, BglII, XbaI and BamHI restriction sites into pBS-β
XhoI
SpeI
BglII
XbaI
BamHI
pβ-Linker
β-globulin intron
DNA Linkers
Step 4:Insertion of SV40 pA in pβ-Linker
BamHI
XhoI
SpeI
BglII
XbaI
BamHI
pβ-Linker-SV40

Figure 8 (continued)

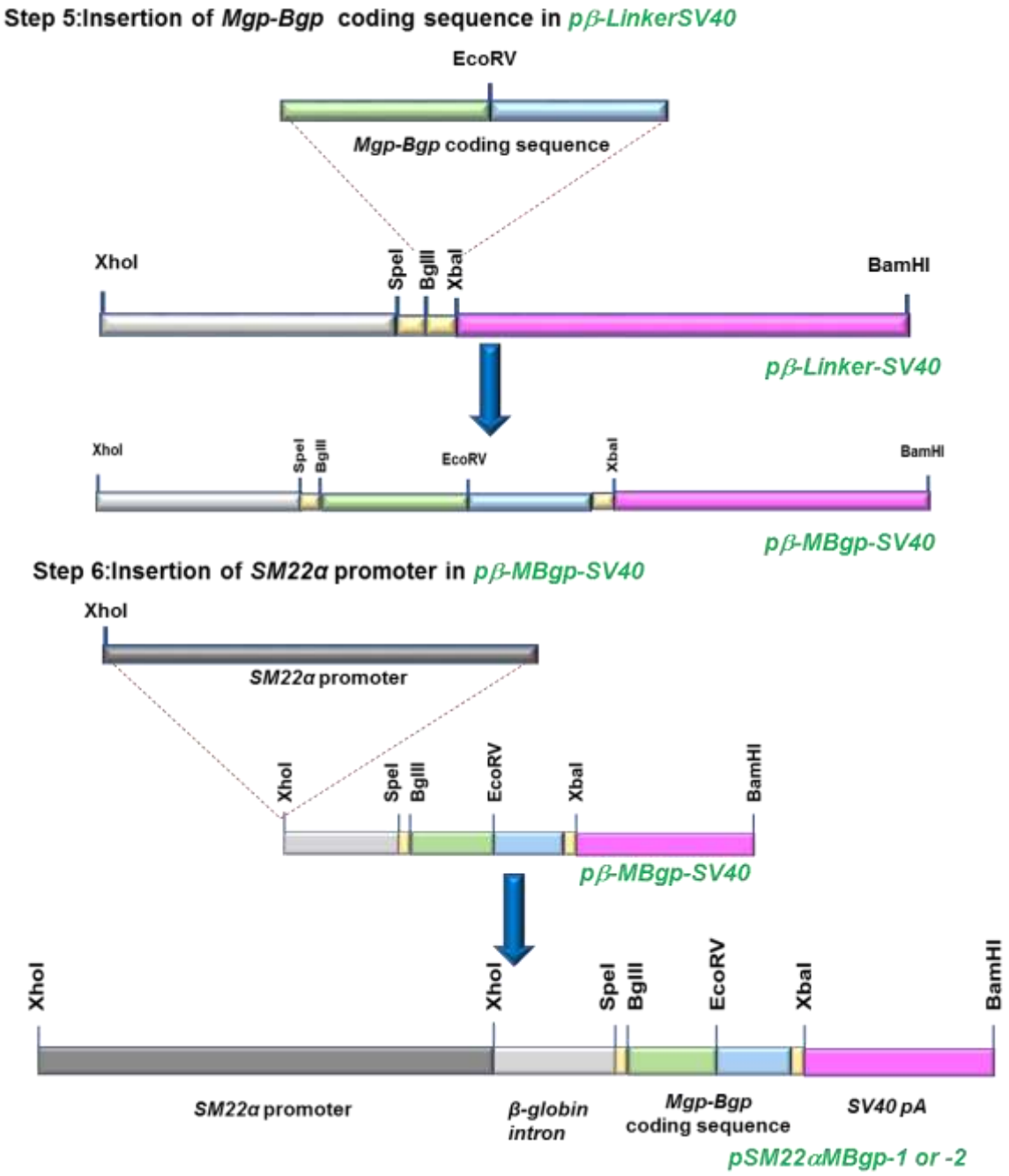

Figure 8: Transgene construction. Flow chart showing the steps to generate transgene constructs *pSM22αMBgp-1 and pSM22αMBgp-2 (Drawings were not to the scale).*

Figure 9

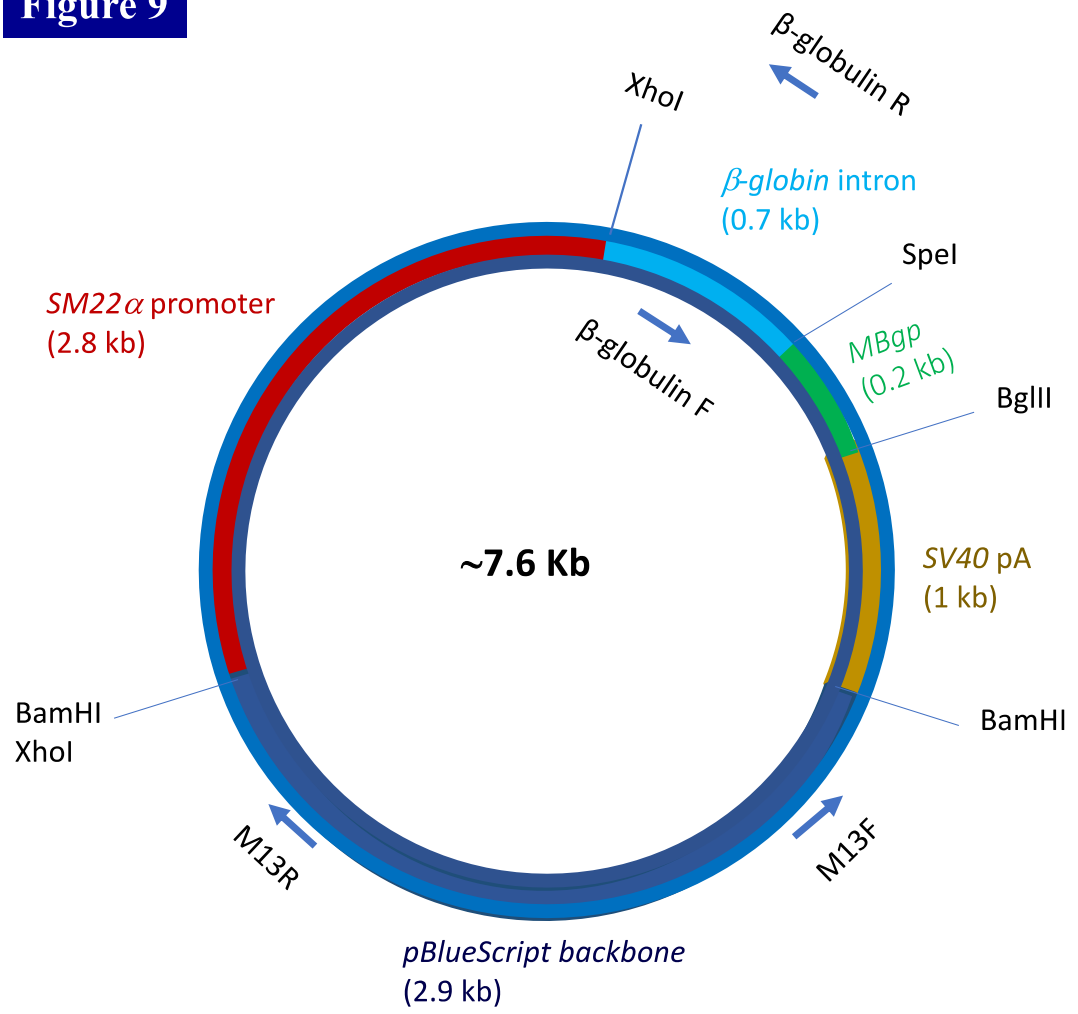

Figure 9: Schematic presentation of *pSM22αMBgp-2.* The map shows the whole transgene construct with the vector backbone which is approximately 7.6 Kb. The transgene construct has been sequenced using *β-globulin Intron F, β-globulin Intron R, M13 F and M13 R. The transgene insert can be released by BamHI digestion. Insert will express an MGP-BGP fusion protein carrying the 3N-terminal Serine residues and the mature BGP protein. In case of pSM22αMBgp-1, a 0.3 kb long MBgp* fragment (Spe1-BglII fragment shown in green) was used.

Figure 10

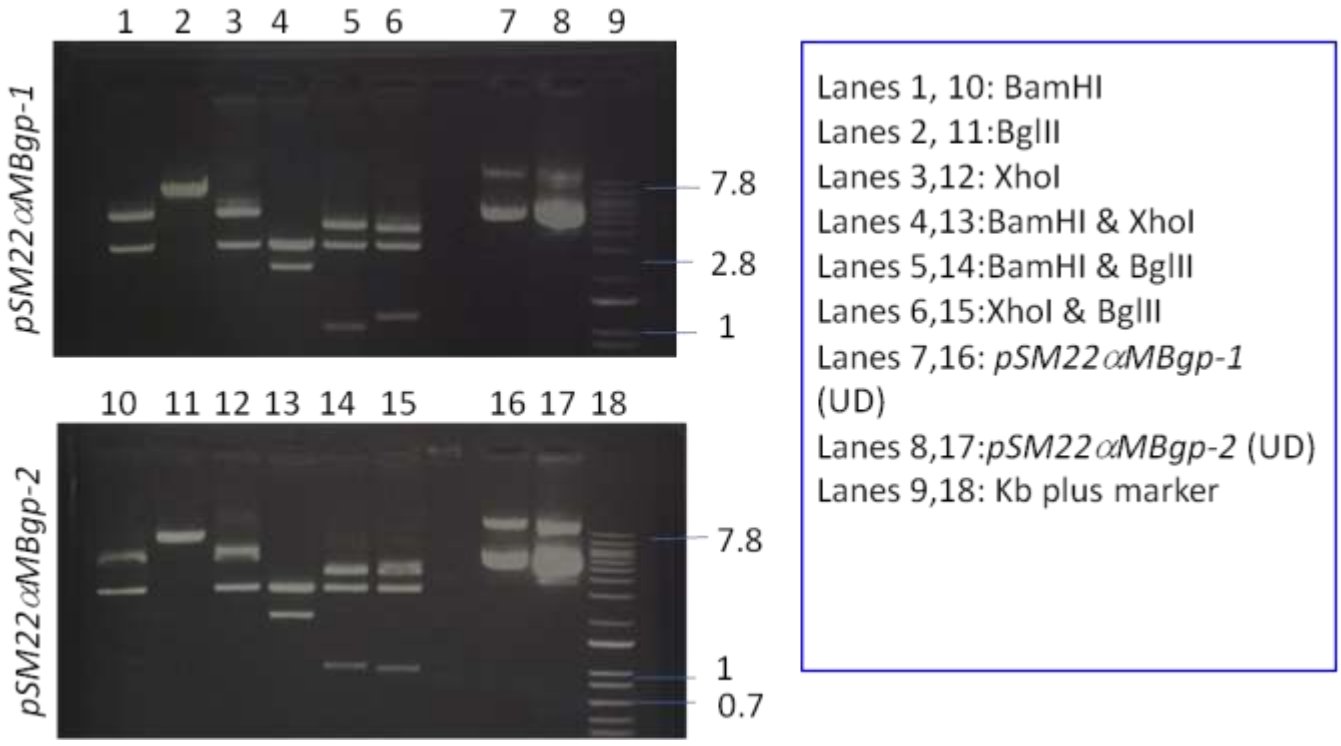

Figure 10: Digestion of *pSM22αMBgp-1 and -2*. Ethidium bromide-stained agarose gels showing the DNA fragments of transgene constructs *pSM22αMBgp-1* (top) *and -2* (bottom)after digestion by the restriction enzymes as indicated in the box. Sizes of some of the fragments in the marker (1 kb plus) have been indicated. UD: undigested DNA

Chapter 5: Discussion

MGP is among the most potent mineralization inhibitors for cartilaginous and vascular tissues [70, 117, 118]. In addition to ectopic cartilage calcification, MGP deficiency causes calcification of vessel walls [65, 69-71, 117, 119], which complicates the prognosis of some vascular diseases. This thesis reports the generation and characterization of a novel MGP-deficient mouse model. This model can be used in future transgenic experiments aimed to determine whether the conserved serine residues are sufficient to confer the anti-mineralization properties of MGP. Towards this end, I have characterized a novel *Mgp* null mouse model and generated two different DNA constructs to express engineered fusion proteins of MGP and osteocalcin.

As described in the Chapter 1, MGP's two sets of post-translational modifications: the conversion of 5 glutamic acid residues (4 in mouse orthologue) to Gla residues, and the phosphorylation of three N-terminal serine residues are thought to be critical for its anti-mineralization functions [96]. The role of Gla residues in MGP's function is already well-supported by both in vitro and in vivo studies [71, 120]. For example, it has been demonstrated that rats treated with warfarin (prevents the enzymatic conversion of Gla residues by blocking the vitamin K oxidation-reduction cycle) [98]. On the other hand, the role of the phosphorylated serine residues in MGP has been studied only in vitro. More recently, our unpublished data demonstrated that serine residues are necessary for MGP's anti-mineralization function in vivo and osteopontin is also another protein which contains serine residues can inhibit ectopic calcification and its inhibitory function mostly depends on serine phosphorylation [96]. However, whether they are sufficient to confer this function to MGP is still unknown. The model and reagents generated in this study will be helpful to address this pending question.

Whether the serine residues are sufficient for MGP's functionality can be examined by expressing the N-terminal domain of MGP carrying the conserved serine residues in fusion with osteocalcin, also known as bone Gla protein (BGP). Osteocalcin/BGP like MGP is a skeletal Gla protein which carries the Gla residues, but not the serine residues [105]. Moreover, despite being a Gla protein, expression of osteocalcin in the vascular walls of MGP-deficient mice did not prevent vascular calcification[71]. These observations form the basis of my hypothesis that an MGP-BGP fusion protein carrying MGP's serine and BGP's glutamic acid residues undergoing γ-carboxylation will show anti-mineralization function.

The above hypothesis can be tested using a conventional transgenic- 'knockout' rescue approach, whereby a desired MGP-BGP fusion protein can be expressed in the arteries of MGP-deficient mice. This compound model is not expected to produce any endogenous MGP, but only the fusion protein specifically expressed in the vascular tissues. Examination of the vascular tissues for ectopic calcification will provide a definitive answer to our research question regarding the anti-mineralization role of the conserved serine residues in MGP. Alternatively, the fusion protein coding sequence can be directly introduced into the *Mgp* locus in a mouse model which can then be expressed under the *Mgp* promoter. This can be achieved by using the CRISPR/Cas9 technique [121]. While the later model is 'avant-garde', faster and will be more suitable for getting the fusion protein expressed in all tissues where native *Mgp* is expressed, there can be some technical difficulties. For example, this approach will require addition of an intron and polyadenylation signal flanking the open reading frame of the transgene in the template sequence (ssODN) [122], which may reduce the efficient targeting resulting in delays in generating the desired mice. Although the cDNA sequence can be directly inserted after the conserved serine

residues of MGP, sometimes following this method, may result in off target effects e.g. insertion and deletion events at the targeted locus or elsewhere [123]. Another drawback is that the modified protein will be driven by MGP promoter and will be expressed in all MGP expressing cells including chondrocytes. If the fusion protein is not secreted and accumulated in chondrocytes it may lead to death of mice. Considering these possible shortcomings, we will pursue the conventional transgenic-'knockout' rescue approach, which have been successfully used many times by our laboratory.

Although MGP 'knockout' model is already available, we took the opportunity to use a newly available mouse strain, that was generated serendipitously while we were attempting to introduce a different mutation in the *Mgp* locus in mice using the CRISPR/Cas9 methods of genetic modifications. Although this new technology has simplified the complexities of genome editing, introduction of such unexpected mutations and 'off-target' effects are common and often considered as a drawback [124, 125]. Since this model was already available while we were conceptualizing the current project, we decided to use it, because it did not carry any neomycin resistant cassette that is present in the *Mgp* locus of the original mutant mice. Considering that the strong phosphoglycerate kinase (PGK) promoter used in the neomycin resistant cassette may affect gene expression [126], our new model can be considered as a 'cleaner' model, with minimum genetic alterations and adverse effects. Such a model will be preferable to 'knock-in' a transgene in the modified *Mgp* locus in future experiments without the possibility of any interference from the neomycin resistance cassette present in the original 'knockout' locus.

During the CRISPR/Cas9-mediated genome editing, a complementary guide RNA determines

the site of double-stranded break in the genomic DNA. In the presence of an external template sequence with flanking homologous sequences (matching the sequences both sides of the break point), this break can be repaired by integrating the template sequence [121]. On the other hand, in the absence of an external template sequence, the ends can be joined by the method of non-homologous end joining. This later process may involve the introduction of random insertion or deletion events, collectively known as 'indels' which can be apparent by DNA sequencing [127]. Indeed, we observed such 'indels' upon sequencing the PCR products generated from $Mgp^{+/\Delta 55\text{-}62}$ mice using the primer pairs specific for the *Mgp* locus. The presence of 'indels' in the heterozygous mice suggests that the modified allele was generating by non-homologous end joining upon the CRISPR/Cas9-mediated double-stranded break. There were additional mutations downstream of the *Δ55-62* mutation, but they were not of any concern as the first mutation generated a stop codon within *Mgp's* open reading frame.

The novel mutation reported here replaced a single nucleotide ($Mgp^{\Delta 55\text{-}62}$) converting the codon for cysteine 19 to a stop codon. Considering that cysteine 19 is the last amino acid of the signal peptide, this modification is expected to result in a small 19 amino acid peptide, but not the rest of the protein. It is however likely that the mutated *Mgp* transcript carrying the premature stop codon will not be stable because of nonsense-mediated decay of such transcripts resulting in no translation [128]. In other words, the modified allele can be considered as a null allele.

The confirmation that the $Mgp^{\Delta 55\text{-}62}$ mutation results in a null allele was further confirmed by our analyses of the mice homozygous for the mutation ($Mgp^{\Delta 55\text{-}62/\Delta 55\text{-}62}$). Indeed, the $Mgp^{\Delta 55\text{-}62/\Delta 55\text{-}62}$ mice appear to recapitulate all the major phenotypic attributes of the original *Mgp-/-* mice

reported by Luo et al [70]. Mice carrying the novel homozygous mutations are smaller and showed medial calcification, two traits seen invariably in all *Mgp-/-* mice. Although our preliminary histological analysis showed a slightly milder vascular calcification phenotype in the former, this needs to be further verified with more mice and side by side analysis. For now, it appears that the presence of the neomycin resistant cassette in the original 'knockout' model does not have any significant effect on the vascular and cartilaginous tissue-associated phenotypes in these mice.

For the current study, I generated two different transgene constructs. Both constructs carry *SM22α* promoter at the 5' end. We have used this promoter previously to successfully drive *Mgp* expression in the VSMCs [129], cell type known for endogenous *Mgp* expression. The promoter sequence is followed by a rabbit β-globin intron sequence for the stability, effective transport and high expression of the transgene [130]. I introduced a chimeric open reading frame that is constituted of the 5' part of mouse *Mgp* open reading frame (coding for the signal peptide and the three conserved serine residues) and a part of the *Bgp* open reading frame (coding the full-length or the mature protein after the proteolytic cleavage). Although BGP is known to be proteolytically cleaved, it is not clear whether this will happen in the VSMCs, the cell type which does not express *Bgp* normally. If the full-length BGP is cleaved in the VSMCs, the availability of these two constructs will allow us to investigate whether the N-terminal MGP peptide with the serine residues will be self-sufficient to prevent vascular calcification by itself or it must have the Gla residues and the extended peptide sequence. Finally, a SV40 polyadenylation signal was added for effective termination of the transgene transcription.

In future, the transgenes can be individually microinjected into the fertilized mouse eggs to generate independent transgenic lines. Upon expression analyses by PCR, suitable founder lines can be mated with $Mgp^{+/\Delta 55\text{-}62}$ mice to express the transgenes in $Mgp^{\Delta 55\text{-}62/\Delta 55\text{-}62}$ mice. The analyses of the arterial tissues of these mice will confirm whether the addition of MGP's N-terminal serine residues to BGP will be sufficient to prevent vascular calcification in these mice. If there is indeed a prevention of vascular calcification by the fusion protein, more detailed analysis will be performed about the possible mechanism(s), e.g. whether net charges, amino acid sequence, all or single serine residues are involved etc. The findings of these experiments will have significant implications as it may promote future studies to determine whether such peptides can be used as therapeutic agents to prevent 'soft' tissue calcification.

Although we established a new, presumably better mouse line, still we cannot guarantee the expression pattern. In addition, the expression pattern specific for vascular smooth muscle cells, still also possible to observe weak, leaky or no expression of the transgene. However, we followed the same strategy to design the construct which has been used by others in the past and they all were successful [69, 71, 131, 132]. Sometimes undesired expression pattern depends on the copy number and insertion site expression level of a transgene. Also, it is possible transgene expression may affect the expression of other genes and cause unrelated phenotype. However, I have established a fresh mouse line and I am expecting the desired expression level and identical phenotypes which will address the concerns raised above.

Chapter 6: Conclusion and Future Effects

We have successfully generated *Mgp*$^{\Delta 55\text{-}62/\Delta 55\text{-}62}$mouse line and also two transgene constructs for future understanding the role of serine phosphorylation of MGP's serine residues specifically in the vascular tissues. From my first objective we got a new *Mgp-/-* model, which unlike the original model, has no neomycin resistant cassette. As mentioned above the presence of a neomycin resistant cassette may affect gene expression in an undesirable way. My preliminary data showing similar traits in the new and original models indicates that the neomycin resistant cassette has no significant effect on the vascular and cartilaginous tissue-associated phenotypes in original mutant mice. In future experiments, we can use the new mutant model to express *Mgp* transgenes such as the constructs reported here.

The constructs generated under my second objective can be used to generate transgenic lines which can be mated with *Mgp*$^{+/\Delta 55\text{-}62}$ mice to express the transgenes in homozygous *Mgp*$^{\Delta 55\text{-}62/\Delta 55\text{-}62}$ mice. The analysis of the arterial tissues of these mice will confirm whether the addition of MGP's N-terminal serine residues to BGP will be sufficient to prevent vascular calcification in these mice. If we demonstrate the functional anti-mineralization role of the fusion protein, future studies to determine whether MGP's N-terminal peptides can be used as therapeutic agents to prevent 'soft' tissue calcification can also be tested. Also, this compound model will serve as a basis for future experiments to investigate how the conserved serine residues and their post-translational modification may affect ECM mineralization. In conclusion, we can say that the proposed transgenic models may help us to open new doors for future clinical therapies or innovation of new drugs for the prevention of vascular calcification.

Chapter 7: References

1. WHO. *Cardiovascular diseases (CVDs)*. 2021.
2. Nair, C., et al., *Cardiovascular disease in Canada.* Health Rep, 1989. **1**(1): p. 1-22.
3. Demer, L.L. and Y. Tintut, *Vascular calcification: pathobiology of a multifaceted disease.* Circulation, 2008. **117**(22): p. 2938-48.
4. Greenland, P., et al., *Coronary artery calcium score combined with Framingham score for risk prediction in asymptomatic individuals.* Jama, 2004. **291**(2): p. 210-5.
5. Kalra, S.S. and C.M. Shanahan, *Vascular calcification and hypertension: cause and effect.* Ann Med, 2012. **44 Suppl 1**: p. S85-92.
6. Wayhs, R., A. Zelinger, and P. Raggi, *High coronary artery calcium scores pose an extremely elevated risk for hard events.* J Am Coll Cardiol, 2002. **39**(2): p. 225-30.
7. Kaipatur, N.R., M. Murshed, and M.D. McKee, *Matrix Gla protein inhibition of tooth mineralization.* J Dent Res, 2008. **87**(9): p. 839-44.
8. Reynolds, J.L., et al., *Human vascular smooth muscle cells undergo vesicle-mediated calcification in response to changes in extracellular calcium and phosphate concentrations: a potential mechanism for accelerated vascular calcification in ESRD.* J Am Soc Nephrol, 2004. **15**(11): p. 2857-67.
9. Frantz, C., K.M. Stewart, and V.M. Weaver, *The extracellular matrix at a glance.* Journal of Cell Science, 2010. **123**(24): p. 4195-4200.
10. Rozario, T. and D.W. DeSimone, *The extracellular matrix in development and morphogenesis: a dynamic view.* Developmental biology, 2010. **341**(1): p. 126-140.
11. Kusindarta, D.L. and H. Wihadmadyatami, *The role of extracellular matrix in tissue regeneration.* Tissue regeneration, 2018. **75728**: p. 6.
12. Abou Neel, E.A., et al., *Demineralization-remineralization dynamics in teeth and bone.* Int J Nanomedicine, 2016. **11**: p. 4743-4763.
13. Jiang, X., et al., *Method development of efficient protein extraction in bone tissue for proteome analysis.* Journal of proteome research, 2007. **6**(6): p. 2287-2294.
14. Alford, A.I., K.M. Kozloff, and K.D. Hankenson, *Extracellular matrix networks in bone remodeling.* Int J Biochem Cell Biol, 2015. **65**: p. 20-31.
15. McKee, M.D., et al., *Extracellular matrix mineralization in periodontal tissues: Noncollagenous matrix proteins, enzymes, and relationship to hypophosphatasia and X-linked hypophosphatemia.* Periodontol 2000, 2013. **63**(1): p. 102-22.
16. Ohtsuka, S., et al., *Chronically decreased aortic distensibility causes deterioration of coronary perfusion during increased left ventricular contraction.* J Am Coll Cardiol, 1994. **24**(5): p. 1406-14.
17. Durham, A.L., et al., *Role of smooth muscle cells in vascular calcification: implications in atherosclerosis and arterial stiffness.* Cardiovasc Res, 2018. **114**(4): p. 590-600.
18. Frismantiene, A., et al., *Smooth muscle cell-driven vascular diseases and molecular mechanisms of VSMC plasticity.* Cell Signal, 2018. **52**: p. 48-64.
19. Bacakova, L., et al., *The role of vascular smooth muscle cells in the physiology and pathophysiology of blood vessels.* Muscle Cell Tissue Curr. Status Res. Field, 2018. **229**.
20. Brozovich, F.V., et al., *Mechanisms of Vascular Smooth Muscle Contraction and the Basis for Pharmacologic Treatment of Smooth Muscle Disorders.* Pharmacol Rev, 2016. **68**(2): p. 476-532.

21. Owens, G.K., M.S. Kumar, and B.R. Wamhoff, *Molecular regulation of vascular smooth muscle cell differentiation in development and disease.* Physiological reviews, 2004. **84**(3): p. 767-801.
22. Chan, P., *Cell biology of human vascular smooth muscle.* Ann R Coll Surg Engl, 1994. **76**(5): p. 298-303.
23. Shi, J., et al., *Metabolism of vascular smooth muscle cells in vascular diseases.* Am J Physiol Heart Circ Physiol, 2020. **319**(3): p. H613-h631.
24. Chistiakov, D.A., I.A. Sobenin, and A.N. Orekhov, *Vascular Extracellular Matrix in Atherosclerosis.* Cardiology in Review, 2013. **21**(6): p. 270-288.
25. Kapustin, A.N., et al., *Calcium regulates key components of vascular smooth muscle cell-derived matrix vesicles to enhance mineralization.* Circ Res, 2011. **109**(1): p. e1-12.
26. Otto, F., et al., *Cbfa1, a candidate gene for cleidocranial dysplasia syndrome, is essential for osteoblast differentiation and bone development.* Cell, 1997. **89**(5): p. 765-71.
27. Mizobuchi, M., D. Towler, and E. Slatopolsky, *Vascular Calcification: The Killer of Patients with Chronic Kidney Disease.* Journal of the American Society of Nephrology, 2009. **20**(7): p. 1453-1464.
28. Franceschi, R.T. and G. Xiao, *Regulation of the osteoblast-specific transcription factor, Runx2: responsiveness to multiple signal transduction pathways.* J Cell Biochem, 2003. **88**(3): p. 446-54.
29. Vattikuti, R. and D.A. Towler, *Osteogenic regulation of vascular calcification: an early perspective.* Am J Physiol Endocrinol Metab, 2004. **286**(5): p. E686-96.
30. Li, Q., Q. Jiang, and J. Uitto, *Ectopic mineralization disorders of the extracellular matrix of connective tissue: molecular genetics and pathomechanisms of aberrant calcification.* Matrix Biol, 2014. **33**: p. 23-8.
31. Herrington, W., et al., *Epidemiology of Atherosclerosis and the Potential to Reduce the Global Burden of Atherothrombotic Disease.* Circ Res, 2016. **118**(4): p. 535-46.
32. Mackey, R.H., L. Venkitachalam, and K. Sutton-Tyrrell, *Calcifications, arterial stiffness and atherosclerosis.* Adv Cardiol, 2007. **44**: p. 234-244.
33. Davignon, J. and P. Ganz, *Role of endothelial dysfunction in atherosclerosis.* Circulation, 2004. **109**(23 Suppl 1): p. Iii27-32.
34. Toussaint, N.D. and P.G. Kerr, *Vascular calcification and arterial stiffness in chronic kidney disease: implications and management.* Nephrology (Carlton), 2007. **12**(5): p. 500-9.
35. Doherty, T.M., et al., *Calcification in atherosclerosis: bone biology and chronic inflammation at the arterial crossroads.* Proc Natl Acad Sci U S A, 2003. **100**(20): p. 11201-6.
36. Boström, K., et al., *Bone morphogenetic protein expression in human atherosclerotic lesions.* J Clin Invest, 1993. **91**(4): p. 1800-9.
37. Askevold, E.T., et al., *Secreted Wnt modulators in symptomatic aortic stenosis.* J Am Heart Assoc, 2012. **1**(6): p. e002261.
38. Alexopoulos, A., et al., *Pathophysiologic mechanisms of calcific aortic stenosis.* Ther Adv Cardiovasc Dis, 2012. **6**(2): p. 71-80.
39. Lee, S.J., I.K. Lee, and J.H. Jeon, *Vascular Calcification-New Insights Into Its Mechanism.* Int J Mol Sci, 2020. **21**(8).

40. Disthabanchong, S. and P. Srisuwarn, *Mechanisms of Vascular Calcification in Kidney Disease.* Adv Chronic Kidney Dis, 2019. **26**(6): p. 417-426.
41. O'Shaughnessy, M.M., et al., *Cause of kidney disease and cardiovascular events in a national cohort of US patients with end-stage renal disease on dialysis: a retrospective analysis.* Eur Heart J, 2019. **40**(11): p. 887-898.
42. Proudfoot, D. and C.M. Shanahan, *Molecular mechanisms mediating vascular calcification: role of matrix Gla protein.* Nephrology (Carlton), 2006. **11**(5): p. 455-61.
43. Goodman, W.G., et al., *Vascular calcification in chronic kidney disease.* Am J Kidney Dis, 2004. **43**(3): p. 572-9.
44. Mizobuchi, M., D. Towler, and E. Slatopolsky, *Vascular calcification: the killer of patients with chronic kidney disease.* J Am Soc Nephrol, 2009. **20**(7): p. 1453-64.
45. Shanahan, C.M., et al., *Arterial calcification in chronic kidney disease: key roles for calcium and phosphate.* Circ Res, 2011. **109**(6): p. 697-711.
46. Nitta, K., *Vascular Calcification in Patients With Chronic Kidney Disease.* Therapeutic Apheresis and Dialysis, 2011. **15**(6): p. 513-521.
47. Fishbein, G.A. and M.C. Fishbein, *Pathology of the Aortic Valve: Aortic Valve Stenosis/Aortic Regurgitation.* Curr Cardiol Rep, 2019. **21**(8): p. 81.
48. Liu, T., et al., *Bicuspid Aortic Valve: An Update in Morphology, Genetics, Biomarker, Complications, Imaging Diagnosis and Treatment.* Front Physiol, 2018. **9**: p. 1921.
49. Wu, B., et al., *Developmental Mechanisms of Aortic Valve Malformation and Disease.* Annu Rev Physiol, 2017. **79**: p. 21-41.
50. Chiyoya, M., et al., *Matrix Gla protein negatively regulates calcification of human aortic valve interstitial cells isolated from calcified aortic valves.* J Pharmacol Sci, 2018. **136**(4): p. 257-265.
51. Di Vito, A., et al., *Extracellular Matrix in Calcific Aortic Valve Disease: Architecture, Dynamic and Perspectives.* Int J Mol Sci, 2021. **22**(2).
52. Hinton, R.B. and K.E. Yutzey, *Heart valve structure and function in development and disease.* Annu Rev Physiol, 2011. **73**: p. 29-46.
53. Li, D.Y., et al., *Elastin is an essential determinant of arterial morphogenesis.* Nature, 1998. **393**(6682): p. 276-80.
54. Li, D.Y., et al., *Novel arterial pathology in mice and humans hemizygous for elastin.* J Clin Invest, 1998. **102**(10): p. 1783-7.
55. Hinton, R.B., et al., *Elastin haploinsufficiency results in progressive aortic valve malformation and latent valve disease in a mouse model.* Circ Res, 2010. **107**(4): p. 549-57.
56. Lee, B., et al., *Linkage of Marfan syndrome and a phenotypically related disorder to two different fibrillin genes.* Nature, 1991. **352**(6333): p. 330-4.
57. Dietz, H.C., et al., *Marfan syndrome caused by a recurrent de novo missense mutation in the fibrillin gene.* Nature, 1991. **352**(6333): p. 337-9.
58. Yuan, S.M. and H. Jing, *Marfan's syndrome: an overview.* Sao Paulo Med J, 2010. **128**(6): p. 360-6.
59. Starman, B.J., et al., *Osteogenesis imperfecta. The position of substitution for glycine by cysteine in the triple helical domain of the pro alpha 1(I) chains of type I collagen determines the clinical phenotype.* J Clin Invest, 1989. **84**(4): p. 1206-14.

60. Brunod, I., et al., *Generalized arterial calcification of infancy with a novel ENPP1 mutation: a case report.* BMC Pediatr, 2018. **18**(1): p. 217.
61. Boyce, A.M., R.I. Gafni, and C.R. Ferreira, *Generalized Arterial Calcification of Infancy: New Insights, Controversies, and Approach to Management.* Curr Osteoporos Rep, 2020. **18**(3): p. 232-241.
62. Khan, T., et al., *ENPP1 enzyme replacement therapy improves blood pressure and cardiovascular function in a mouse model of generalized arterial calcification of infancy.* Dis Model Mech, 2018. **11**(10).
63. Hajjawi, M.O., et al., *Mineralisation of collagen rich soft tissues and osteocyte lacunae in Enpp1(-/-) mice.* Bone, 2014. **69**: p. 139-47.
64. Prosdocimo, D.A., et al., *Autocrine ATP release coupled to extracellular pyrophosphate accumulation in vascular smooth muscle cells.* Am J Physiol Cell Physiol, 2009. **296**(4): p. C828-39.
65. Munroe, P.B., et al., *Mutations in the gene encoding the human matrix Gla protein cause Keutel syndrome.* Nat Genet, 1999. **21**(1): p. 142-4.
66. Keutel, J., G. Jörgensen, and P. Gabriel, *[A new autosomal-recessive hereditary syndrome. Multiple peripheral pulmonary stenosis, brachytelephalangia, inner-ear deafness, ossification or calcification of cartilages].* Dtsch Med Wochenschr, 1971. **96**(43): p. 1676-81 passim.
67. Perrone, E., et al., *A Novel MGP Gene Mutation Causing Keutel Syndrome in a Brazilian Patient.* Mol Syndromol, 2018. **9**(3): p. 159-163.
68. Khosroshahi, H.E., et al., *Long term follow-up of four patients with Keutel syndrome.* Am J Med Genet A, 2014. **164a**(11): p. 2849-56.
69. Khavandgar, Z., et al., *Elastin haploinsufficiency impedes the progression of arterial calcification in MGP-deficient mice.* J Bone Miner Res, 2014. **29**(2): p. 327-37.
70. Luo, G., et al., *Spontaneous calcification of arteries and cartilage in mice lacking matrix GLA protein.* Nature, 1997. **386**(6620): p. 78-81.
71. Murshed, M., et al., *Extracellular matrix mineralization is regulated locally; different roles of two gla-containing proteins.* J Cell Biol, 2004. **165**(5): p. 625-30.
72. Leroux-Berger, M., et al., *Pathologic calcification of adult vascular smooth muscle cells differs on their crest or mesodermal embryonic origin.* J Bone Miner Res, 2011. **26**(7): p. 1543-53.
73. Jono, S., et al., *Phosphate regulation of vascular smooth muscle cell calcification.* Circ Res, 2000. **87**(7): p. E10-7.
74. Chen, N.X., et al., *Phosphorus and uremic serum up-regulate osteopontin expression in vascular smooth muscle cells.* Kidney Int, 2002. **62**(5): p. 1724-31.
75. Lomashvili, K.A., et al., *Phosphate-induced vascular calcification: role of pyrophosphate and osteopontin.* J Am Soc Nephrol, 2004. **15**(6): p. 1392-401.
76. Lomashvili, K.A., et al., *Upregulation of alkaline phosphatase and pyrophosphate hydrolysis: potential mechanism for uremic vascular calcification.* Kidney Int, 2008. **73**(9): p. 1024-30.
77. Heiss, A., et al., *Structural basis of calcification inhibition by alpha 2-HS glycoprotein/fetuin-A. Formation of colloidal calciprotein particles.* J Biol Chem, 2003. **278**(15): p. 13333-41.

78. Bunton, T.E., et al., *Phenotypic alteration of vascular smooth muscle cells precedes elastolysis in a mouse model of Marfan syndrome.* Circ Res, 2001. **88**(1): p. 37-43.
79. Starcher, B.C. and D.W. Urry, *Elastin coacervate as a matrix for calcification.* Biochem Biophys Res Commun, 1973. **53**(1): p. 210-6.
80. Seligman, M., R.F. Eilberg, and L. Fishman, *Mineralization of elastin extracted from human aortic tissues.* Calcif Tissue Res, 1975. **17**(3): p. 229-34.
81. Price, P.A. and M.K. Williamson, *Primary structure of bovine matrix Gla protein, a new vitamin K-dependent bone protein.* J Biol Chem, 1985. **260**(28): p. 14971-5.
82. Cancela, M.L., et al., *Matrix Gla protein in Xenopus laevis: molecular cloning, tissue distribution, and evolutionary considerations.* J Bone Miner Res, 2001. **16**(9): p. 1611-21.
83. Laizé, V., et al., *Evolution of matrix and bone gamma-carboxyglutamic acid proteins in vertebrates.* J Biol Chem, 2005. **280**(29): p. 26659-68.
84. Cancela, M.L., V. Laizé, and N. Conceição, *Matrix Gla protein and osteocalcin: from gene duplication to neofunctionalization.* Arch Biochem Biophys, 2014. **561**: p. 56-63.
85. Hale, J.E., M.K. Williamson, and P.A. Price, *Carboxyl-terminal proteolytic processing of matrix Gla protein.* J Biol Chem, 1991. **266**(31): p. 21145-9.
86. Murshed, M., et al., *Unique coexpression in osteoblasts of broadly expressed genes accounts for the spatial restriction of ECM mineralization to bone.* Genes & development, 2005. **19**(9): p. 1093-1104.
87. Yao, Y., et al., *Inhibition of bone morphogenetic proteins protects against atherosclerosis and vascular calcification.* Circ Res, 2010. **107**(4): p. 485-94.
88. Khavandgar, Z., et al., *Elastin haploinsufficiency impedes the progression of arterial calcification in MGP-deficient mice.* Journal of Bone and Mineral Research, 2014. **29**(2): p. 327-337.
89. Bhatia, P.V., et al., *Apert's syndrome: Report of a rare case.* J Oral Maxillofac Pathol, 2013. **17**(2): p. 294-7.
90. Chokdeemboon, C., et al., *FGFR1 and FGFR2 mutations in Pfeiffer syndrome.* J Craniofac Surg, 2013. **24**(1): p. 150-2.
91. Paliga, J.T., et al., *Premature closure of the spheno-occipital synchondrosis in Pfeiffer syndrome: a link to midface hypoplasia.* J Craniofac Surg, 2014. **25**(1): p. 202-5.
92. Goldstein, J.A., et al., *Earlier evidence of spheno-occipital synchondrosis fusion correlates with severity of midface hypoplasia in patients with syndromic craniosynostosis.* Plast Reconstr Surg, 2014. **134**(3): p. 504-510.
93. Cancela, L., et al., *Molecular structure, chromosome assignment, and promoter organization of the human matrix Gla protein gene.* J Biol Chem, 1990. **265**(25): p. 15040-8.
94. Bashir, A., et al., *Coronary Artery Calcium Assessment in CKD: Utility in Cardiovascular Disease Risk Assessment and Treatment?* Am J Kidney Dis, 2015. **65**(6): p. 937-48.
95. Price, P.A., J.D. Fraser, and G. Metz-Virca, *Molecular cloning of matrix Gla protein: implications for substrate recognition by the vitamin K-dependent gamma-carboxylase.* Proc Natl Acad Sci U S A, 1987. **84**(23): p. 8335-9.
96. Schurgers, L.J., et al., *Post-translational modifications regulate matrix Gla protein function: importance for inhibition of vascular smooth muscle cell calcification.* J Thromb Haemost, 2007. **5**(12): p. 2503-11.

97. Luo, G., et al., *The matrix Gla protein gene is a marker of the chondrogenesis cell lineage during mouse development.* J Bone Miner Res, 1995. **10**(2): p. 325-34.
98. Price, P.A., S.A. Faus, and M.K. Williamson, *Warfarin causes rapid calcification of the elastic lamellae in rat arteries and heart valves.* Arterioscler Thromb Vasc Biol, 1998. **18**(9): p. 1400-7.
99. Price, P.A., S.A. Faus, and M.K. Williamson, *Warfarin-induced artery calcification is accelerated by growth and vitamin D.* Arterioscler Thromb Vasc Biol, 2000. **20**(2): p. 317-27.
100. Farzaneh-Far, A., et al., *Vascular and valvar calcification: recent advances.* Heart, 2001. **85**(1): p. 13-7.
101. Stehbens, W.E., *The hypothetical epidemic of coronary heart disease and atherosclerosis.* Med Hypotheses, 1995. **45**(5): p. 449-54.
102. Price, P.A., *Gla-containing proteins of bone.* Connect Tissue Res, 1989. **21**(1-4): p. 51-7; discussion 57-60.
103. Dumitru, N., et al., *The Link Between Bone Osteocalcin and Energy Metabolism in a Group of Postmenopausal Women.* Curr Health Sci J, 2019. **45**(1): p. 47-51.
104. Price, P.A., J.W. Poser, and N. Raman, *Primary structure of the gamma-carboxyglutamic acid-containing protein from bovine bone.* Proc Natl Acad Sci U S A, 1976. **73**(10): p. 3374-5.
105. Viegas, C.S., et al., *Sturgeon osteocalcin shares structural features with matrix Gla protein: evolutionary relationship and functional implications.* J Biol Chem, 2013. **288**(39): p. 27801-11.
106. Hinoi, E., et al., *An Osteoblast-dependent mechanism contributes to the leptin regulation of insulin secretion.* Ann N Y Acad Sci, 2009. **1173 Suppl 1**: p. E20-30.
107. Karsenty, G. and M. Ferron, *The contribution of bone to whole-organism physiology.* Nature, 2012. **481**(7381): p. 314-20.
108. Oury, F., et al., *Osteocalcin regulates murine and human fertility through a pancreas-bone-testis axis.* J Clin Invest, 2013. **123**(6): p. 2421-33.
109. Ducy, P., et al., *Increased bone formation in osteocalcin-deficient mice.* Nature, 1996. **382**(6590): p. 448-52.
110. Price, P.A., J.S. Rice, and M.K. Williamson, *Conserved phosphorylation of serines in the Ser-X-Glu/Ser(P) sequences of the vitamin K-dependent matrix Gla protein from shark, lamb, rat, cow, and human.* Protein Sci, 1994. **3**(5): p. 822-30.
111. Wajih, N., et al., *Processing and transport of matrix gamma-carboxyglutamic acid protein and bone morphogenetic protein-2 in cultured human vascular smooth muscle cells: evidence for an uptake mechanism for serum fetuin.* J Biol Chem, 2004. **279**(41): p. 43052-60.
112. O'Young, J., et al., *Matrix Gla protein inhibits ectopic calcification by a direct interaction with hydroxyapatite crystals.* J Am Chem Soc, 2011. **133**(45): p. 18406-12.
113. Hackeng, T.M., et al., *Total chemical synthesis of human matrix Gla protein.* Protein Sci, 2001. **10**(4): p. 864-70.
114. Li, H., et al., *Applications of genome editing technology in the targeted therapy of human diseases: mechanisms, advances and prospects.* Signal Transduct Target Ther, 2020. **5**(1): p. 1.

115. Koo, T., et al., *Selective disruption of an oncogenic mutant allele by CRISPR/Cas9 induces efficient tumor regression.* Nucleic Acids Res, 2017. **45**(13): p. 7897-7908.
116. Torres-Ruiz, R. and S. Rodriguez-Perales, *CRISPR-Cas9 technology: applications and human disease modelling.* Brief Funct Genomics, 2017. **16**(1): p. 4-12.
117. El-Maadawy, S., et al., *Cartilage formation and calcification in arteries of mice lacking matrix Gla protein.* Connect Tissue Res, 2003. **44 Suppl 1**: p. 272-8.
118. Schurgers, L.J., et al., *Characteristics and performance of an immunosorbent assay for human matrix Gla-protein.* Clin Chim Acta, 2005. **351**(1-2): p. 131-8.
119. Weaver, K.N., et al., *Keutel syndrome: report of two novel MGP mutations and discussion of clinical overlap with arylsulfatase E deficiency and relapsing polychondritis.* Am J Med Genet A, 2014. **164a**(4): p. 1062-8.
120. Parashar, A., et al., *Elastin calcification in in vitro models and its prevention by MGP's N-terminal peptide.* J Struct Biol, 2021. **213**(1): p. 107637.
121. Doudna, J.A. and E. Charpentier, *Genome editing. The new frontier of genome engineering with CRISPR-Cas9.* Science, 2014. **346**(6213): p. 1258096.
122. Cong, L. and F. Zhang, *Genome engineering using CRISPR-Cas9 system.* Methods Mol Biol, 2015. **1239**: p. 197-217.
123. Li, J., et al., *Efficient inversions and duplications of mammalian regulatory DNA elements and gene clusters by CRISPR/Cas9.* Journal of molecular cell biology, 2015. **7**(4): p. 284-298.
124. Peng, R., G. Lin, and J. Li, *Potential pitfalls of CRISPR/Cas9-mediated genome editing.* Febs j, 2016. **283**(7): p. 1218-31.
125. Fu, Y., et al., *High-frequency off-target mutagenesis induced by CRISPR-Cas nucleases in human cells.* Nat Biotechnol, 2013. **31**(9): p. 822-6.
126. Pham, C.T., et al., *Long-range disruption of gene expression by a selectable marker cassette.* Proc Natl Acad Sci U S A, 1996. **93**(23): p. 13090-5.
127. Wang, H., et al., *One-step generation of mice carrying mutations in multiple genes by CRISPR/Cas-mediated genome engineering.* Cell, 2013. **153**(4): p. 910-8.
128. Karamyshev, A.L. and Z.N. Karamysheva, *Lost in Translation: Ribosome-Associated mRNA and Protein Quality Controls.* Front Genet, 2018. **9**: p. 431.
129. Marulanda, J., et al., *Prevention of arterial calcification corrects the low bone mass phenotype in MGP-deficient mice.* Bone, 2013. **57**(2): p. 499-508.
130. Buchman, A.R. and P. Berg, *Comparison of intron-dependent and intron-independent gene expression.* Mol Cell Biol, 1988. **8**(10): p. 4395-405.
131. Marulanda, J., et al., *Matrix Gla protein deficiency impairs nasal septum growth, causing midface hypoplasia.* J Biol Chem, 2017. **292**(27): p. 11400-11412.
132. Marulanda, J. and M. Murshed, *Role of Matrix Gla protein in midface development: Recent advances.* Oral Dis, 2018. **24**(1-2): p. 78-83.